Factors affecting CD4 T cell recognition of the EBV-encoded tumour antigen EBNA1

By Henry Leonard

UNIVERSITY OF BIRMINGHAM

A thesis submitted to the University of Birmingham for the degree of MRes in Cancer Sciences

School of Cancer Research
College of Medical and Dental Sciences
University of Birmingham

Word count: 14,527

August 2014

Abstract

Epstein-Barr virus (EBV) is associated with 200,000 cases of cancer per year. Although these include B cell lymphomas and epithelial carcinomas, the ability of T cells specific to viral antigens to target the latter, which constitute the majority of cases, has not been explored. In this study I have investigated the processing and CD4 T cell recognition of epithelial cells expressing EBNA1, a virally-encoded protein expressed in all EBV-associated malignancies. EBNA1 was equally stable in B cells and epithelial cells but EBNA1-specific CD4 T cell clones were nevertheless able to recognise both types of target cell. The potential effects of EBV-encoded micro-RNA BART18 on autophagy and CD4 T cell recognition were examined and showed that the loss of BART18 increased the autophagy levels of EBV-positive Jijoye Burkitt lymphoma cells under nutrient starvation conditions. Finally, the effects of a pharmacological inhibitor of EBNA1 dimerisation, JLP2, on the viability and T cell recognition of EBV-positive B cells was also investigated. JLP2 did not increase CD4 T cell recognition but transiently decreased the viability of one of two EBV-positive lymphoblastoid cell lines coincident with this line's uptake of the drug.

Acknowledgements

Thanks must go to Graham, for supervision and even the occasional meeting throughout the year. It has truly been a wonderful start to my research career in cancer immunology.

The technical support and seemingly endless supply of knowledge provided by Tracey has been invaluable. Working alongside you and Alex, who would have also imparted sage wisdom if it hadn't been for the hood fans drowning out his mumbling, has been very enjoyable.

To my colleagues and friends that I have made in Cancer Sciences; Anna, Bens (French and Anna's), Calum, Kristina, Laura, Luke, Nenad and Olivia. I thank you for the discussions, coffee breaks and basketball games we have shared.

For providing valuable resources to the project I would also like to thank Leah and Chris.

Thank you to Ann, for providing the funds that facilitated my mastering of Cancer Science, and Paul, for helping me keep a roof over my head.

Finally, all of the thanks must go to Anna. I am sure that without you the grammatical integrity of this thesis would have been severely compromised and many meals may have been missed in the pursuit of perfection. Luckily, I have found my perfection, Anna, thank you.

Table of contents

1. Introduction

1.1 T cell Immunology

Human T lymphocytes (T cells) provide adaptive cellular immunity, protecting the host by destroying or suppressing cells that have been infected with a virus or have become cancerous. More than 11% of all cancers are associated with viral infections [1] and therefore virus-specific antigens are being studied as potential therapeutic targets.

1.1.1 T cells

T cells are lymphocytes that possess a T cell receptor (TCR) and play a central role in controlling virally infected or cancerous cells [2]. The TCR consists of a heterodimer, typically α and β chains [3], which associates with a CD3 molecule to form a functional TCR complex. During development within the thymus, a T cell will generate a distinct TCR and start expressing either CD4 or CD8 [4, 5]. The TCRs are generated through hyper-somatic mutations of the variable (V), diversity (D) and joining (J) genes. This process involves the combination of various segments from the locus of each of these genes, allowing a large number of possible combinations. Because the gene recombination processes occurs in an almost random fashion (although not entirely random [6]), a vast diversity of TCRs can be created within the T cell population, allowing for the recognition of virtually any non-self antigen. For the β chain of the TCR, the D region binds to a J segment followed by a V region. There are also constant domains within this formation, which act as hinges and transmembrane regions [7]. The α chain recombination follows the same process as the β rearrangement, but without the inclusion of a D region. The α and β chains form a heterodimer superdomain that constitutes the peptide-binding site of the αβ-TCR. For both MHC class I and II molecules, the β-sheet represents the base of

the binding groove, which is straddled by α-helixes. However, there are important distinctions to be made between the CD4 and the CD8 T cells MHC peptide-binding domains that explains their functional dichotomy. The peptide-binding site of MHC class I molecules (α1α2) has a single polymorphic heavy chain, associated to the light chain sub-unit (β2-microglobulin). This closed conformation typically binds peptides that are 8-10 amino acids long. Whereas the peptide-binding site of MHC class II molecules (α1β1) has two heavy chains, which creates an open ended groove that typically holds peptides of 12 to 20 amino acids in length [8]. T cells are activated by short peptides, epitopes, which are displayed by MHC molecules. Normally this initial activation will come from antigen presenting cells (APC) [9, 10].

Subsets of T cells, characterised by the expression of different cell surface markers, have different effector functions once activated. Generally, CD8 T cells act as cytotoxic T lymphocytes (CTLs) that produce cytokines, such as interferon-γ (IFNγ) and tumour necrosis factor-α (TNF-α), performing cytolytic activity that can directly kill a target cell. CD4 T cells can be subdivided into several subsets based on the expression of effector cytokines. The most studied subset, Th1 cells, produce IFNγ, TNF, interleukin-2 (IL-2) and lymphotoxin-α (LTa), which can act to stimulate other immune cells such as macrophages and other T cells [11]. Th2 T cells, activated by IL-4, provide immunity against extracellular parasites and release effector cytokines such as IL-4, IL-10 and IL-13. The Th1-Th2 paradigm provides a simplified framework for the signalling molecules and cytokines involved in functional differentiation. However, there is evidence that this distinctions in not simply a static relationship. For instance, Th1 cells can be converted into Th2 cells upon re-stimulation with IL-4 [12] and Th2 cells can be made to have additional Th1 function upon IL-12 stimulation [13]. The functional flexibility of CD4 T cell activity is thought to arise from genetic plasticity of the differentiation programs [14]. Interestingly, there are a cut-off point for differentiation. Irreversible fixation of T cell subtype can arise in long-term populations,

after the cells have undergone a certain number of divisions [12]. There are also certain functional transitions that do not occur, such as the conversions from a Th1 or Th2 cell into a Treg cell. For the purposes of this work I have purely focussed on Th1 CD4 T cells. Classically, CD8 T cells were presumed to control cancer growth. Recently however, the importance of the previously overlooked CD4 T cells has become apparent. Multiple reports have demonstrated that CD4 T cells exhibit cytotoxic function and have the ability to induce senescence within malignant cells [15, 16].

1.1.2 Generation of T cell epitopes by antigen processing and presentation

T cells recognise short peptide fragments, termed epitopes, which are bound in the groove of MHC class I or MHC class II molecules and displayed on a cell's surface. A crucial factor in cellular immunity is the generation and display of epitopes through antigen processing and presentation. Proteins within the cytoplasm are continuously being broken down and recycled, two main mechanisms involved being proteasomal degradation and autophagy. From both of these degradation pathways epitopes are generated, which can then enter into the antigen processing pathways [17, 18]. Epitopes bound to MHC molecules are trafficked to the cell's surface for presentation to the immune system. Immunogenic proteins, derived from mutations or intracellular parasites, are non-self and therefore elicit an immune response upon presentation. This process allows T cells to selectively eliminate the cancerous or virus infected target cells. MHC class I molecules are recognised by CD8 T cells and are expressed by almost all nucleated cells. In contrast, MHC class II molecules are recognised by CD4 T cells and, whilst it was initially thought that MHC class II was limited to subsets of specialised APCs, they are now known be expressed on a wide range of cells given the appropriate conditions. For example, exposure to certain inflammatory cytokines, such as IFNγ, activates the MHC class II transactivator CIITA, leading to the upregulation of MHC class II presentation in many cell types

[19]. Therefore, numerous cell types are potentially visible to CD4 T cells, especially within the inflammatory tumour microenvironment.

The classical model for antigen processing and presentation states that endogenous proteins are processed by the proteasome and presented by MHC class I, while exogenous proteins are endocytosed and then presented by MHC class II. However, this simplified model has had to be revised following two important observations: i) exogenous proteins can be processed and presented via MHC class I (e.g. cross presentation by dendritic cells) [20] and ii) endogenous proteins contribute to a significant proportion of the epitopes presented by MHC class II (e.g. proteins processed by autophagy) [21].

1.1.3 Antigen processing and presentation by autophagy

One of the main routes allowing intracellular proteins to gain access to the MHC class II processing pathway is macroautophagy (hereafter referred to as autophagy). This pathway is an evolutionarily conserved homeostatic mechanism in eukaryotes by which old or damaged proteins are degraded and recycled [22]. The highly coordinated process of autophagy involves the formation of a double membrane, known as an autophagosome, around cytosolic cargo, which is then transported to lysosomes for degradation [23]. In most cells a low basal level of autophagy is maintained. However, in times of cellular stress, such as nutrient deprivation, it is upregulated to postpone the cell's death from starvation. Autophagy was initially thought to be a non-selective pathway, but more recent evidence suggests that distinct microstructures are directly targeted for destruction [24]. Importantly for the present study, intracellular proteins that are degraded by autophagy gain access to the MHC class II processing pathway through the MHC class II loading compartments (MIICs), as evident from the several autophagy dependent antigens that stimulate CD4 T cell recognition [25]. Experimentally, higher levels of MHC class II

antigen presentation is seen upon activation of autophagy by starvation [21]. Furthermore, fusing together a target antigen with LC3, an autophagy protein that localises to the autophagosome, dramatically increases the levels of MHC class II presentation and CD4 T cell recognition [26, 27]. Autophagy therefore provides an important mechanism for pathogenic proteins to be endogenously processed and presented to CD4 T cells.

1.1.4 Immunology and immunotherapy of virus-associated malignancies

Cells that have become cancerous or infected with viruses can be controlled by adaptive immune surveillance, such as T cell recognition of immunogenic epitopes [28, 29]. Virus-associated malignancies can arise when the immune system is suppressed, but they can also develop in people who are not overtly immunosuppressed. Oncogenic viruses, such as EBV and HPV, have co-evolved with humans and have developed immune evasive tactics, helping the infected cells avoid immune detection [30]. As oncogenic viruses account for over 11% of all malignancies [1], there is considerable interest in targeting viral epitopes, which are not present in normal tissue, for treating these cancers.

Recently, the immunotherapy of cancer has progressed with the development of several clinically effective treatments. These include; immune checkpoint blockade, such as ipilimumab, and passive cellular immunotherapy, such as adoptive T cell transfer. Administering T cells, which have their own immunological activity, offers a therapy to patients that may not have fully functional immune system themselves [31]. It is well known that CD8 T cells are effective for antitumour immunity, while CD4 T cells have generally been overlooked as only providing a support role for sustained immune response [32]. However, recent evidence has shown that CD4 T cells are able to provide effector function and induce senescence in tumour cells [16]. This is supported by evidence from clinical trials of post-transplant lymphoproliferative disorder

(PTLD) patients, in which a positive correlation was shown between an increased CD4:CD8 T cells ratio and improved patient outcome [33]. Further evidence for the importance of CD4 T cells comes from melanoma, where CD4 T cells were able to clear tumours resistant to CD8 T cells in a mouse model [34] and administering CD4 T cells was able to completely eradicated tumours in patients [35]. Although previously overlooked, CD4 T cells clearly have considerable potential to enhance the efficacy of cancer immunotherapies. In this regard, viral malignancies provide a valuable model system in which to develop novel immunotherapeutic strategies. The fact that the virally encoded tumour antigens are completely restricted to only the tumour cells minimises the risk of dangerous off target immune responses. Furthermore, because the target antigens are non-self, this means that the T cell responses are typically of a higher avidity compared to most other tumour-associated antigens.

1.2 Epstein-Barr virus

Epstein-Barr virus (EBV) is a DNA tumour virus that has co-evolved with the human species for millions of years and infects over 90% of adults worldwide [36]. As a lifelong herpesvirus infection, EBV normally persists asymptomatically due to effective control by T cell surveillance [37]. The initial oral transmission of EBV leads to a primary infection of epithelial cells within the oropharynx where the virus enters a lytic phase, replicating in vast quantities. The latent phase of EBV infection, mainly found in memory B cells and certain epithelial types, involves the persistence of the viral episome without active viral production [38]. Different latency stages are characterised by various patterns of virally-encoded miRNA and latent gene expression [39].

1.2.1 EBV-associated cancers

The transformative properties of EBV's latent protein expression act synergistically with tumorigenic traits that may develop within a host cell. For example, LMP1 and LMP2 are responsible for enhancing cell proliferation programs and EBNA1 has been shown to enhance tendencies for cell immortalisation [40] [41]. EBV infections are associated with around 200,000 malignancies worldwide every year [42]. In B cell lymphomas, EBV is associated with 45% of Hodgkin's lymphoma (28,000) and 90% of Burkitt's lymphoma (6,600) cases within endemic areas. However, the majority of cases are found in the epithelial cancers where EBV is associated with around 10% of gastric carcinoma (84,000 cases) and 97% of nasopharyngeal carcinoma (NPC) (78,000) cases. Targeting a viral antigen common to all these diseases may therefore offer a universal treatment option for these patients.

T cells play an important role in controlling EBV infections and mitigating the development of the associated cancers. This is highlighted by evidence from patients who are immunosuppressed after organ transplantation and develop PTLD. This virus-associated malignancy arises due to

the removal of T cell surveillance, leading to the uncontrolled proliferation of EBV infected B cells. Recently, clinical trials have shown successful results from EBV-specific immunotherapy. In a Phase II clinical trial, 14 out of 33 PTLD patients made a complete remission after receiving adoptive T cell therapy [33]. This paper also demonstrated that improved outcomes could be achieved with a higher CD4:CD8 T cells ratio and by appropriating closer HLA matched donors. Another example of an EBV targeted immunotherapy of cancer is a poxvirus vaccine currently in phase II testing, delivering a LMP2-EBNA1 fusion protein designed to stimulate autologous T cells against latent EBV-associated NPC [43]. Potentially, improvements could be made in the field of immunotherapy by better understanding the utility of different T cell phenotypes and EBV antigen presentation, in order to find the most appropriate effectors and universal target on which to focus further research.

1.3 Epstein-Barr virus nuclear antigen 1

The expression of EBV nuclear protein antigen 1 (EBNA1) is seen in 100% of EBV-associated malignancies, as it has vital roles in maintaining the viral episome during cell division [44]. It is now known that intracellular processing results in MHC presentation of epitopes, which elicits responses from CD4 and CD8 T cells [45, 46]. However, a definitive mechanism explaining the endogenous processing of EBNA1 and the precise links to MHC presentation is yet to be fully elucidated.

1.3.1 Stability

The endogenous stability of EBNA1 has mainly been studied in EBV infected B cells, known as lymphoblastic cell lines (LCLs), in which EBNA1 has a very long half-life. Autophagy has been suggested as one of the mechanisms for the low levels of degradation that do occur. Evidence for this comes from the inhibition of lysosomal acidification, which results in the accumulation of EBNA1 in cytosolic autophagosomes and reduces CD4 T recognition levels of certain MHC class II EBNA1 epitopes [25].

Interestingly, the one study that has examined the stability of EBNA1 in another cell type, epithelial cells, reported that its half-life was much shorter **(Figure 1.3.1)** [47]. The half-life of EBNA1 was measured in B cells and epithelial cell lines (transiently transfected with a plasmid encoding EBNA1) by inhibiting protein synthesis with cycloheximide and measuring the level of EBNA1 over time. As expected, the half-life of EBNA1 in B cells was very long, greater than 30h. However, EBNA1 was degraded rapidly in epithelial cell lines; the half-life was calculated to be around 4h in the HaCaT cell line and 20–24h for SVMR6 and HEK293 cell lines. The half-life of EBNA1 was not affected by removing the glycine/alanine repeat (GAr) domain sequence (EBNA1ΔGA) or by inhibiting proteasomal degradation (which was successful in blocking CD8 T

cell recognition). This work raises some interesting questions regarding MHC class II processing of EBNA1, which have not yet been explored within the literature, such as the mechanism responsible for the enhanced degradation seen in cell types other than B cells. This mechanism could potentially be autophagy, which would supply EBNA1 peptides to the MHC class II processing pathway, perhaps making EBV-associated epithelial malignancies excellent targets for CD4 T cells. This knowledge could have potential applications for the immunotherapy of EBV-associated epithelial malignancies.

1.3.2 Endogenous processing and presentation

Although there is no consistent intracellular processing route for the MHC class II antigens of EBNA1 [36, 48], the presentation of several epitopes has been shown to be autophagy dependent [25, 49]. A study by Leung and colleagues demonstrated that only two (SNP and VYG) out of the three CD4 T cell clones tested against LCLs could recognise their target and that only one of these epitopes (SNP) was dependent on autophagy for presentation [45]. The overexpression of EBNA1 did not alter the processing route, but the relocalisation of EBNA1 to the cytoplasm resulted in all three of the epitopes being processed effectively by autophagy. This work demonstrates that the natural nuclear location of EBNA1 benefits the protein by conferring protection from autophagic degradation and consequently limiting CD4 T cell recognition.

1.3.3 T cell recognition of latent antigens

CD8 T cell recognition of EBNA1 is limited by the small number of MHC class I epitopes present in the protein [36, 50]. Comparatively, CD4 T cells are able to recognise a wide range of EBNA1 epitopes presented by MHC class II. The Th1 CD4 T cells that respond to EBNA1 epitopes are capable of producing IFNγ and have been shown to effectively kill B cells infected with EBV [51].

Many EBV-associated malignancies are capable of expressing MHC class II molecules, including Burkitt's lymphoma (which actually lacks MHC class I) and even the epithelial cells associated with EBV infection, which can typically upregulate MHC class II expression in the presence of cytokines that are present in the inflammatory tumour microenvironment. It is therefore vital to study the novel area of CD4 T cells controlling EBV-associated epithelial malignancies.

1.3.4 Inhibition of EBNA1 function

Another complementary therapeutic strategy to treat EBV-associated malignancies is the inhibition of EBNA1, which is essential for the maintenance of the viral episome and is expressed in all EBV-associated malignancies. Mutant dominant-negative EBNA1 proteins affect EBNA1 processing and increase the levels of epitope presentation by MHC class I, thereby enhancing T cell recognition [52]. However, the logistics of using dominant-negative proteins as a therapeutic treatment is technically challenging [53] and a simpler approach may be to utilise pharmacological inhibitors of EBNA1 dimerisation. Peptides that bind specifically to the EBNA1 dimerisation domain are selective agents that inhibit EBNA1 function and, through removal of the EBV episome, could also help induce cell death of EBV infected cells. It is not known whether these drugs will also affect the processing and presentation of EBNA1. Several advancements have recently been made in the development of such an EBNA1 inhibitor that could potentially be used to treat EBV-associated malignancies [54, 55].

JLP2 is an EBNA1 specific probe, designed using molecular computation to inhibit EBNA1 dimerisation [55]. The presence of the JL chromophore allows the molecule to be visualised with a confocal microscope and fluorescence levels quantified with flow cytometry. Upon binding to EBNA1 the emission spectrum of JLP2 is enhanced, facilitating a direct comparison between

EBV and non-EBV infected cells. *In vitro,* the treatment of an EBV-positive NPC cell line, in comparison to treatment of an EBV-negative cell line, with JLP2 allowed for selective visualisation and induced a dose dependent decrease in cell viability [55]. As there may be clinical use for a pharmacological inhibitor of EBNA1 in the immunotherapy of EBV-associated malignancies, it is worth exploring the effect of JLP2 in different cell types and to determine whether this inhibition of dimerisation will also impact the EBNA1-epitopes presentation to T cells.

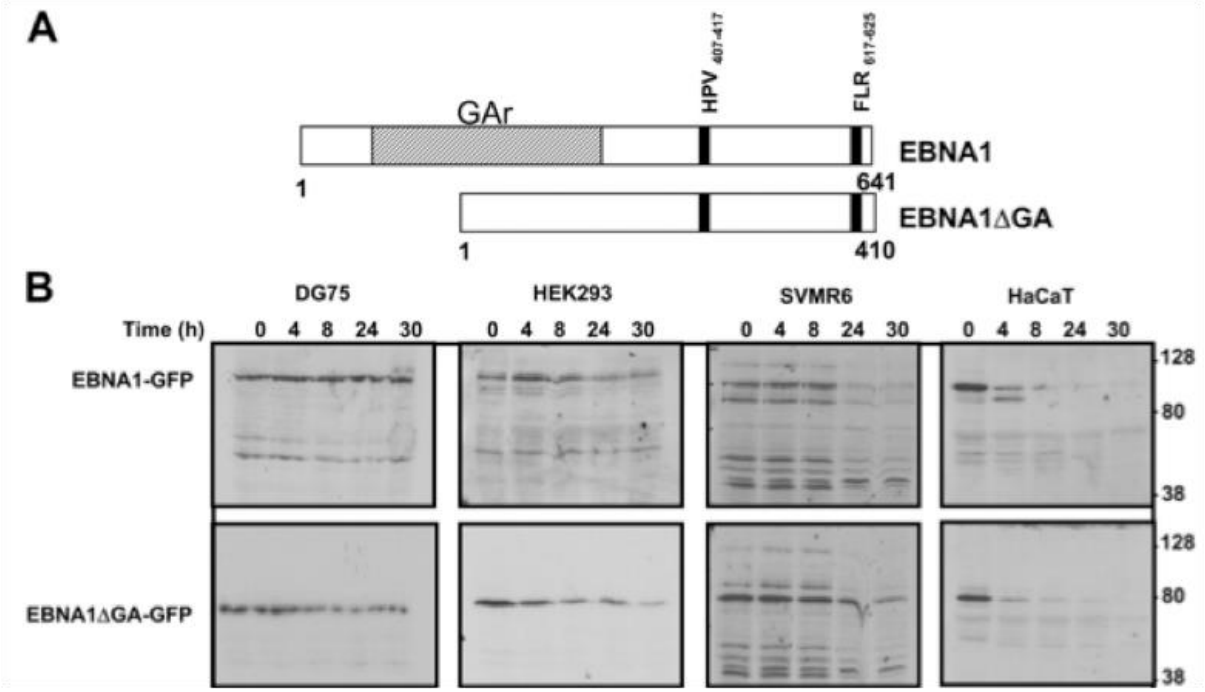

Figure 1.3.1 Variable half-life of EBNA1 in epithelial cell lines
A) A schematic map of EBNA1 and EBNA1ΔGA expression constructs (B) Intracellular half-life of transfected EBNA1/EBNA1ΔGA in different cell types. After the addition of cycloheximide (50µg/ml) EBNA1 was chased for 30h and expression levels were measured using western blot. DG75 (B cell) shows EBNA1 to be incredibly stable over 30h. However, HEK293 epithelial cells, SVMR6 keratinocytes and HaCaT keratinocytes all have a much shorter half-life for EBNA1. Figure taken from Tellam J. *et al*. J Exp Med 2004;199:1421-1431 [47]

1.4 Aims of this project

The aim of this project was to explore the processing and presentation of the ubiquitously expressed EBV-encoded EBNA1 protein in the context of epithelial cancers. To achieve this, the half-life of EBNA1 was assessed and the CD4 T cell recognition of several epithelial cell lines was measured. This project also aimed to explore the manipulation of CD4 T cell recognition through the application of an EBNA1 dimerisation inhibitor (JLP2) and through the knockout of a specific EBV-encoded miRNA (BART 18), postulated to suppress autophagy levels. The work here was designed to gain further insight into the utility of EBNA1 specific CD4 T cells, with the long term aim of developing immunotherapeutic options for patients with EBV-associated epithelial malignancies.

2. Materials and methods

2.1 Cell lines

2.1.1 Table of all the adherent cell lines used in the study

Cell line	Cell type	Source	Split ratio
MKN1	Gastric carcinoma	Chris Dowson (1)	1:5
MKN28	Gastric carcinoma	Chris Dowson	1:5
MKN45	Gastric carcinoma	Chris Dowson	1:5
NUGC4	Gastric carcinoma	Chris Dowson	1:3
SNU	Gastric carcinoma	Chris Dowson	1:3
HeLa	Epithelial	Graham Taylor (1)	1:6
293FT	Epithelial	Leah Fitzsimmons (1)	1:8
HaCaT	Karanocyte	Graham Taylor	1:6
MJS	Melanoma	Graham Taylor	1:8
MJS EV overexpression	Melanoma	Marjolein Hooykaas (2)	1:5
MJS B16 overexpression	Melanoma	Marjolein Hooykaas	1:5
MJS B18 overexpression	Melanoma	Marjolein Hooykaas	1:5
MJS C1 overexpression	Melanoma	Marjolein Hooykaas	1:5

Key:
1) University of Birmingham
2) University of Leiden

2.1.2 Table of all the B cell lines used in the study

Cell line	Cell type	Source	Split ratio
LCL (GT)	EBV+ B cell	Graham Taylor (1)	1:2
LCL (GS)	EBV+ B cell	Graham Taylor	1:2
Akata	EBV- B cell	Alison Leese (1)	1:3
Awaia	EBV- B cell	Alison Leese	1:3
Jijoye EV k/o	EBV+ Burkitt's lymphoma	Marjolein Hooykaas (2)	1:2
Jijoye B16 k/o	EBV+ Burkitt's lymphoma	Marjolein Hooykaas	1:2
Jijoye B18 k/o	EBV+ Burkitt's lymphoma	Marjolein Hooykaas	1:2

Key:
1) University of Birmingham
2) University of Leiden

Lymphoblastic cell lines (LCLs) provided by the lab were B cells previously immortalised through the infection with EBV (strain B95.8 strain prototype type I).

2.2 Resources

2.2.1 Table of reagents

Reagents	Details	Storage	Manufacturer
RPMI (media)	RPMI-1640 supplemented with 0.2M L-glutamine	4°C	Gibco
FCS	Foetal calf serum (FCS)	-20°C	Gibco
pen/strep	Penicillin-streptomycin (5000IU/ml penicillin and 5000µg/ml streptomycin solution)	4°C	Gibco
Opti-MEM	Reduced-Serum Medium	4°C	Life technologies
PBS	Phosphate buffered saline solution (1 PBS tablet/100ml SDW)	RT	Oxoid
PBS Tween	PBS + Tween (0.5ml/L for ELISA, 1ml/L for Western blot)	RT	Dulbecco
Dox	Doxycycline (100µg/ml) dissolved in DMSO	4°C	Sigma
Cycloheximide	Cycloheximide (100mg/ml) dissolved in DMSO	4°C	Sigma
Lipofectamine	Lipofectamine 2000	4°C	Life technologies
Mirus	Mirus Transit X2	4°C	Mirus bio
Propidium Iodide		RT	Life technologies
WST-1		-20°C	Roche
IFN-γ	Recombinant IFN-γ	-20°C	Peprotech
TMB		4°C	Oxoid
ExtrAvidin-Peroxidase		4°C	Life technologies
Coating buffer	12mM Sodium carbonate and 74mM Potassium Bicarbonate pH9.2	RT	

Blocking buffer	PBS-Tween (BSA)	4°C	
Run buffer	250mM Tris,1.9M Glycine and 1% SDS	RT	
Sample buffer	62.5mM Tris pH6.8, 4% SDS and 0.01% Bromophenol blue,	4°C	
Urea buffer	9M Urea and 50mM Tris pH7	RT	
JLP1	5mM JLP1 dissolved in DMSO	-20°C	
JLP2	JLP2 5mM dissolved in DMSO	-20°C	

2.2.2 Table of kits

Kit	**Details**	**Storage**	**Manufacturer**
BCA protein assay kit	Reagents A:B (20:1)	4°C	Thermoscientific
ECL western blot detection reagents	Reagents 1:2 (1:1)	4°C	GE healthcare

2.2.3 Table of antibodies

Detection	Primary	Secondary	Technique
EBNA1 (50-70kDa)	1H4 (1:50)	Anti-Rat (1:000)	Western blot
LC3-II (14kDa)	LC3 (1:3000)	Anti-Goat (1:000)	Western blot
Cyclin E (53kDa)	Cyclin E (1:300)	Anti-Goat (1:000)	Western blot
Cyclin D2 (34kDa)	Cyclin D2 (1:300)	Anti-Goat (1:000)	Western blot
BIP (64kDa)	BIP (1:1000)	Anti-Rat (1:000)	Western blot
IFNγ	Anti-Human IFNγ capture	Biotinylated Anti-Human IFNγ	ELISA
MHC class I	Anti-Human HLA-ABC	NA	Flow cytometry
MHC class II	Anti-Human HLA-DR	NA	Flow cytometry

All antibodies were stored at -20ºC. The western blot antibodies were diluted (ratios given in table) in 5ml of 5% milk.

2.2.4 Plasmids

All plasmids used for the transfection of adherent cell lines had been previously developed within the laboratory (G. Taylor, University of Birmingham) and were built upon a pCDNA3 backbone. These induced: EBNA1 constructs, HLA-restriction genes, and a GFP plasmid. The various EBNA1 constructs, E1ΔGA, E1ΔNLSk/o and IiE1Δ, each possessed different capabilities of accessing MHC class II processing pathway **(Figure 2.2.1** for details).

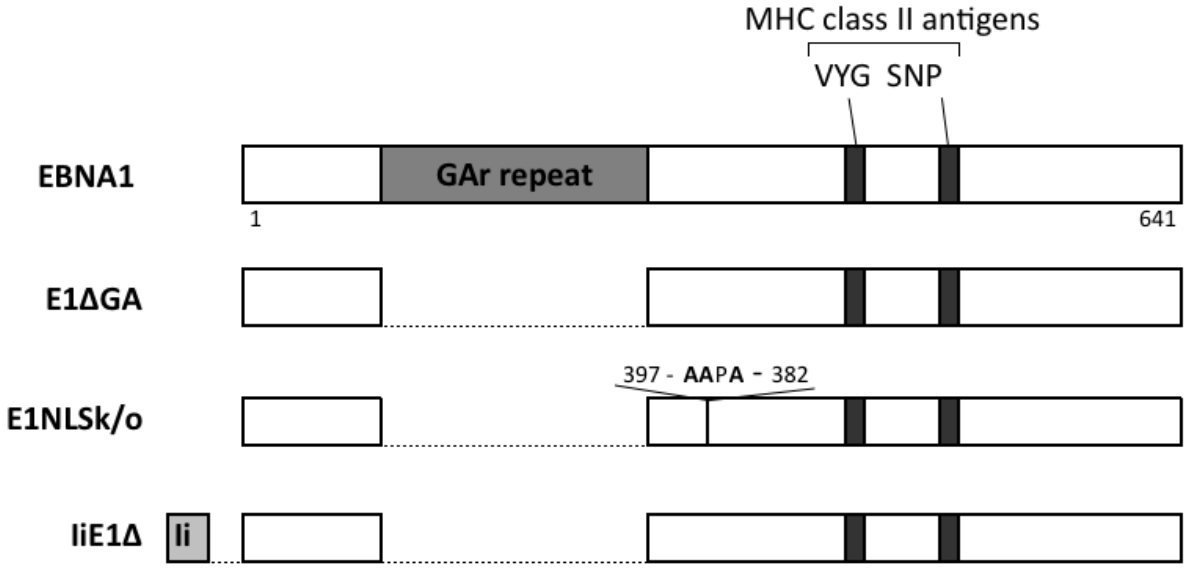

Figure 2.2.1 Schematic of EBNA1 constructs

A schematic map of the various EBNA1 constructs, which had previously been incorporated into a pCDNA3 vector for use in transient transfection. A full length EBNA1 is shown at the top with annotated locations of GAr and two MHC class II-restricted epitopes, SNP and VYG. E1ΔGA, which has the GAr repeat entirely deleted, is shown below. Next, E1ΔNLSk/o is shown to be identical to E1ΔGA except for the mutation of 3 amino acids within the nuclear localisation sequences (resulting in a cytoplasmic-localised EBNA1). Finally the IiE1Δ is shown, which is identical to the E1ΔGA apart from the addition of an invariant chain sequence (amino acids 1-80) to the amino terminal end of the protein (resulting in effective transport of EBNA1 into the MHC class II processing pathway).

2.3 Techniques

2.3.01 Cell culture

All cell lines were cultured (37^{o}C 5% CO_2) in T75 flasks (Corning) and passaged twice a week depending on confluence (see Table 2.1.1 for split ratio). All adherent cell lines were cultured in RPMI 10% FCS and 1% pen/strep. All non-adherent (B cell) lines were cultured in RPMI 10% FCS. All adherent cell lines were passaged by removing media from the flask, washing twice with 6ml PBS and adding 1ml of trypsin for 5-10 minutes (37^{o}C 5% CO_2). Loose cells were then suspended in fresh media and split in the same way as non-adherent cells by passaging the cells at the required ratio.

2.3.02 Fluorescent microscopy

The same area of cells was visualised (80x) using a microscope (Evos) under bright field and UV.

2.3.03 Lentiviral transduction

Adherent cells ($2x10^5$) were cultured (37^{o}C 5% CO_2) in 6 well plates for 24h. The infectious lentiviral supernatant (harvested from lentivirus construction in 293FT cells) and polybrene (6µg/ml) were added to the cells, which were then incubated (37^{o}C 5% CO_2) for 30 minutes. The plate was then centrifuged (2,200rpm) for 2h at 32^{o}C. The supernatant was removed from the cells, which were then washed twice with 2ml of PBS. Fresh media was added and normal culturing was resumed. The lentiviral gene integration was assessed by measuring the levels of GFP expression 21 days after the transduction.

2.3.04 Transient transfections

2.3.04.1 Lipofectamine 2000 transfection

Adherent cells ($6x10^5$) were cultured (37ºC 5% CO_2) in 6 well plates for 24h (typically reaching 80% confluency before the transfection). Lipofectamine (5µl/well) was mixed with pre-warmed opti-MEM (150µl/well) for 5 minutes (room temperature). DNA (various possible concentrations 0.2-4µg/ml) was then combined with the lipofectamine and additional opti-MEM (150µl/well). This transfection solution was incubated (room temperature) for 25 minutes. The media within the 6 well plates was replaced by 200µl/well opti-MEM and 300µl/well of transfection solution. The cells were then incubated (37ºC 5% CO_2) for 4h (rocked every 30 minutes). The transfection solution was then replaced with fresh media and the transfected cells were cultured for 2-3 days before use. (The volumes of transfection reagents were adjusted accordingly for larger or smaller well sizes)

2.3.04.2 Mirus TransIT-X2 transfection

Adherent cells ($3x10^5$) were cultured (37ºC 5% CO_2) in 12 well plates for 12h (typically reaching 80% confluency before the transfection). DNA (1µg/well), TransIT-X2 (3µl/well) and pre-warmed Opti-MEM (250µl/well) were mixed and then incubated (room temperature) for 30 minutes. 250µll of this transfection solution was pipetted gently onto the cells (without removing the original media) and the plates were rocked to achieve even distribution. The cells were cultured (37ºC 5% CO_2) for at least 24h before use.

2.3.05 LC3 flux

The cell lines were cultured (37ºC 5% CO_2) in four wells of a 6 well plate for 24h. The media was replaced, using normal media (10% FCS) for two wells and serum free media (0% FCS) for the

other two. For both serum conditions, one of the two wells was treated with bafilomycin A1 (100nM). After 6h incubation (37^{o}C 5% CO_2) the cells were harvested and washed twice in PBS (5ml). After the final centrifuge (1500rpm for 5 minutes) the PBS was removed using a p1000 pipette and the cell pellet was stored (-80^{o}C) until use in western blots.

2.3.06 Protein stability assay

Adherent cells were cultured in four wells of a 6 well plate for 48h after transient transfection with an EBNA1 plasmid. Cycloheximide (50µg/ml) was added to the wells and the cells were chased for 0, 4, 8 or 24h. The cells were harvested and washed twice in PBS (5mls). After the final centrifuge (1500rpm for 5 minutes), the PBS was removed using a p1000 pipette and the cell pellet was stored (-80^{o}C) until use in western blots.

2.3.07 SDS-PAGE and western blotting

The cell pellet was suspended in urea buffer (1µl per 1x10^{4} cells) and sonicated (Qsonica) at 30% for 10 seconds. The sample was then centrifuged at 13,000rpm for 20 minutes (4^{o}C). The supernatant was transferred to a sterile eppendorf (1.5ml) and protein concentration was determined using a BCA protein assay. The standardised samples were combined with 2X Gel Sample Buffer and β-mercaptoethanol (1:20µl) within a fume hood. The tubes were heated to 100^{o}C for 5 minutes on a heat block before the samples were loaded onto an Any kD Precast Gel (Bio-Rad) and run at 100-150V for 1-2h. In some cases a ChemiDoc (Bio-Rad) was used to analyse the protein loading of the gel. The protein was then transferred from the gel onto a nitrocellulose membrane (Midi Trans-Blot Turbo transfer pack (Bio-Rad)) using a Trans-blot Turbo Transfer system. The membrane was then blocked with milk (5% milk in PBS-Tween) for 1h. The relevant primary antibody (see Table 2.2.3) was then incubated (4^{o}C) with the membrane on a 3D rocker for 12h. The membrane was washed (10 minutes on a 3D rocker at

room temperature) four times in PBS-Tween and then the secondary antibody incubated (room temperature) with the membrane on a 3D rocker for 1h. The membrane was washed (10 minutes on a 3D rocker at room temperature) four times in PBS-Tween and then treated using the ECL kit (for western blot detection), after which the film was exposed to the membrane within a cassette. The film was developed using an automatic film developer, then the protein ladder on the membrane was aligned and marked onto the film. In some cases, after ECL treatment a ChemiDoc was used as an alternative to film development to measure the band intensities.

2.3.08 BCA protein assay

Protein lysate samples were diluted (1:2 and 1:4) using urea buffer and 20µl was added in duplicate to a 96 flat bottom plate. A protein standard (BSA 2-0.125mg/ml using half dilution method) was then added to the 96 flat bottom plate, also in duplicate. The WR reagent was prepared (50:1 A:B regents from BCA kit for protein assays) and 200µl/well was added to the plate. The plate was incubated (37^{o}C 5% CO_2) for 30 minutes. Absorbance (550nm) was then measured using a plate reader. The protein standard curve allowed the protein concentration for each sample to be determined. The original samples were then standardised (diluted using urea buffer) to the equivalent protein concentrations for use in SDS-PAGE.

2.3.09 MHC class I and II staining

Each cell line was cultured (37^{o}C 5% CO_2) for 3 days in two T25 flasks; one with IFNγ (10-100ng/ml) and the other left untreated. The cells were harvested by trypsinisation and resuspended in PBS (1% FCS). The cells were split ($4x10^5$) into three FACS tubes, centrifuged (1,750rpm) and, with the supernatant removed, incubated (37^{o}C 5% CO_2) for 30 minutes. One of the FACS tubes was treated with 20µl of the MHC class I specific antibody (antihuman (W6/32) HLA-ABC), the next was treated with 5µl of the MHC class II specific antibody (antihuman

(L243) HLA-DR) and the third FACS tube was left untreated. The cells were incubated on ice for 60mins (flicked every 20mins), washed twice in 3mls PBS (1%FCS) and finally resuspended in 200µl of PBS for use in flow cytometry. The levels of surface MHC presentation were measured using flow cytometry (FL-4) as the antibodies were conjugated to APC.

2.3.10 Propidium iodide staining

The control, containing both dead (freeze thawed) and living cells, was prepared. After adding propidium iodide (life technologies) to each of the controls and the samples (to make a final concentration of 3µM), the cells were immediately analysed using flow cytometry (FL-3). The gating around the living and dead cells in the control allowed accurate assessment of viable cells within each sample.

2.3.11 Flow cytometry

Cell samples (suspended in PBS) were vortexed before being analysed with a flow cytometer (Accuri C6). The number of cells used, FL measurement and gating depended on the specific experiment.

2.3.12 T cell assay

T cells ($5x10^3$/well) were incubated (37°C 5% CO_2) with target cells ($5x10^4$/well) in a 96 well round bottom plate with 200µl RPMI (10% FCS) for 12h. The supernatant was harvested and the IFNγ levels were measured using an ELISA.

2.3.13 ELISA

A flat bottom 96 well Coat MaxiSorp plate (Nunc) was coated with anti-human IFNγ capture (50µl/well) diluted in coating buffer (0.75µg/ml) for 12h at 4°C. Coating buffer was flicked off and

the plate was blocked with blocking buffer (200µl/well) for 1h. The plate was washed (with PBS-Tween) six times and then the standards (50µl/well, ranging from 4000–68.5pg/ml) and supernatant samples (50µl/well) from the overnight T cell assay were added to the plate (in triplicate). The plate was incubated at room temperature for 4h and then washed six times (with PBS-Tween). Biotin-labeled anti-human IFNγ (50µl/well) was diluted (1/1333) in blocking buffer, added to the plate and incubated (room temperature) for 2h. The plate was washed six times (with PBS-Tween). ExtrAvidin-Peroxidase (50µl/well) was diluted (1/1000) in blocking buffer and added to the plate, which was then incubated (room temperature) for 30min. The plate was washed eight times (with PBS-Tween) before adding TMB substrate (100µl/well) for 20 minutes to allow for colour development. The reaction was stopped using 1M HCL (100µl/well). The absorbance (450nm) of the samples was assessed using a plate reader. The IFNγ standard curve allowed the level of IFNγ from the T cell assay samples to be calculated.

3. Results

3.1 Endogenous stability of EBNA1

Cell lines were chosen that have physiological relevance to EBV-associated epithelial malignancies, in which to study the endogenous stability of EBNA1. Several gastric carcinoma cell lines were selected; MKN1, MKN28, MKN45 and NUGC4. Additionally, various model cell lines were also chosen based on their use in previous studies; 293FT (epithelial) and HaCaT (Keratinocyte, specialised epithelial) cell lines that had been used to report the low stability of EBNA1 and HeLa (epithelial) and MJS (melanoma) cell lines that had been used for the study of antigen processing and presentation. The MKN28 cell line was natively EBV-positive and therefore expressed physiological levels of EBNA1. In order to study the endogenous stability of EBNA1 in the various cell lines, I decided that it would be worthwhile spending the time and resources to establish an inducible EBNA1 expression system, in which physiological or indeed supraphysiological levels of EBNA1 could be generated on demand.

3.1.1 Lentiviral transduction of epithelial lines with EBNA1

A lentiviral transduction system was chosen to generate stable cell lines with a heritable EBNA1 gene incorporated into the host cells' genome. The lentiviral system I selected had been previously developed and optimised for the transduction of B cells (L. Fitzsimmons, personal communication). The lentiviral construct consisted of an inducible full length EBNA1 and a constitutively expressed GFP gene. The infectious lentivirus was produced in 293FT cells, harvested and used in the transduction of epithelial cell lines; MKN1, MKN28 MKN45, HeLa and HaCaT.

To determine whether the lentiviral genome had been stably incorporated into the cell lines, microscopy **(Figure 3.1.1)** and flow cytometry **(Figure 3.1.2)** were used to assess GFP expression 21 days after transduction. A high proportion of cells were successfully transduced for the MKN1 (96.1%) and MKN28 (86.9%) cell lines, with lower levels seen in the MKN45 (60.9%), HaCaT (50.0%) and Hela (31.9%) cell lines.

To assess the amount of protein expressed from the inducible EBNA1 gene, a doxycycline (dox) titration was performed on the lentivirus transduced MKN1 cell line. The MKN1 cells were cultured with dox (0, 10, 20, 50, 100 or 200ng/ml) for 48h. The cells were then harvested and the protein levels standardised. The EBNA1 protein levels were measured using a western blot **(Figure 3.1.3)**. The inducible EBNA1 gene was seen to be expressed in the absence of dox and, although the cells had been effectively transduced, high doses of dox only induced low levels of EBNA1 expression. This inducible expression of EBNA1 was low in comparison to the levels seen in lentiviral transduced B cells or even physiological levels seen in naturally EBV-positive cell lines, such as LCL and MKN28 cells (data not shown).

Although EBNA1 expression was only inducible to low levels a stability assay was attempted, measuring the natural degradation of EBNA1 in the lentivirus transduced cell lines (MKN1 and MKN28). The cells were treated with dox (200ng/ml) for 48h to induce EBNA1 expression. Protein synthesis was then inhibited with the addition of cycloheximide (50µg/ml) and cells were chased for 0, 4, 8 or 24h. Protein levels were standardised and EBNA1 levels were assessed using a western blot **(Figure 3.1.4)**. Despite the low expression of EBNA1, the consistent bands seen over 24h, in both MKN1 and MKN28, suggested that the full length EBNA1 was stable and not subject to degradation. Although the other lentivirus transduced cell lines were tested several times, the induced EBNA1 levels were too low to provide data from western blot analysis.

The reason for the low inducible EBNA1 expression in the lentivirus transduced epithelial cells was not investigating further. Instead, an alternative method of expressing EBNA1 in epithelial cells was explored.

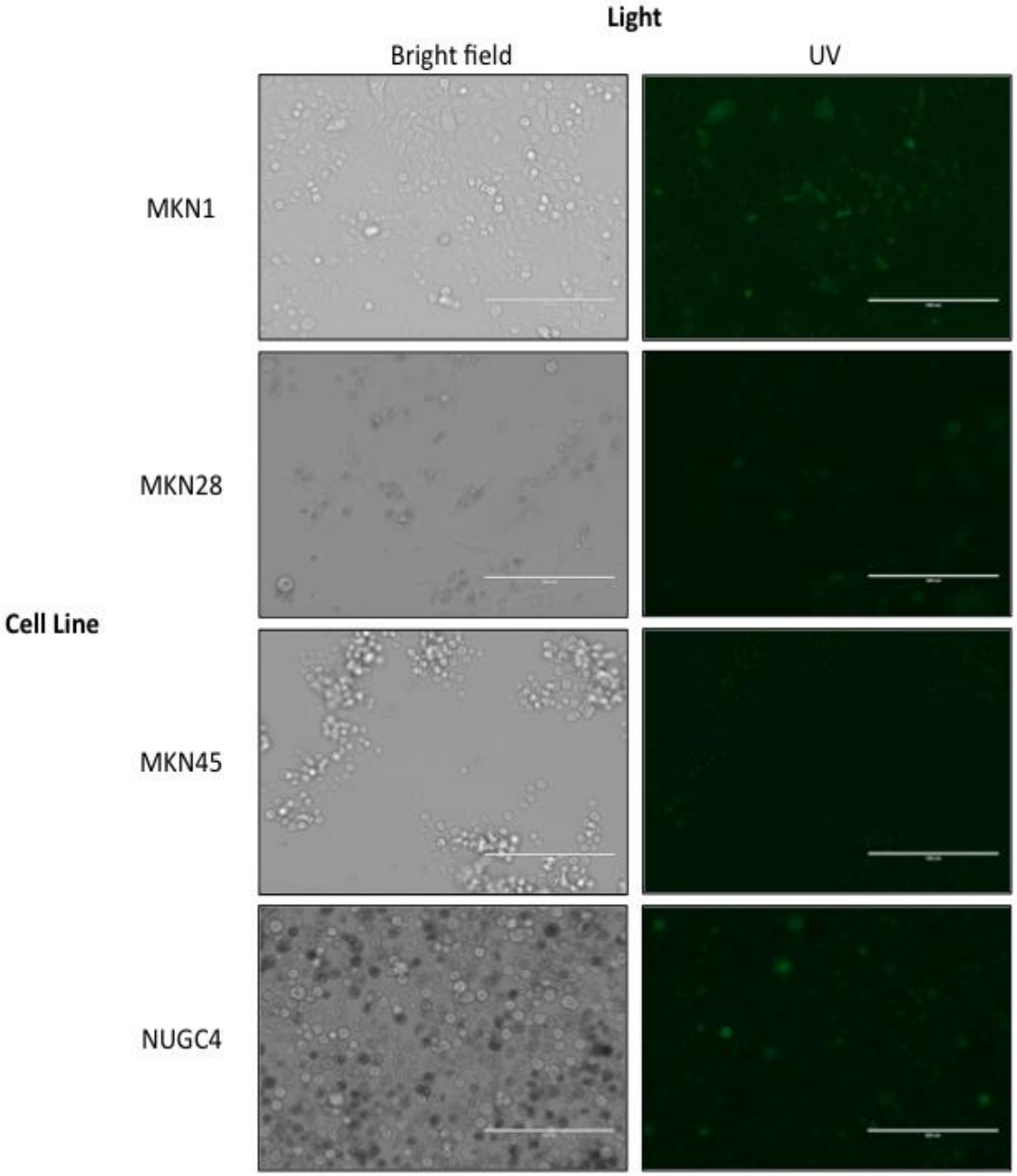

Figure 3.1.1 Visualisation of GFP expression in lentivirus transduced epithelial cell lines
Fluorescent microscopy was used to examine cell lines (MKN1, MKN28, MKN45 and NUGC4) transduced with lentivirus expressing the inducible EBNA1 and constitutive GFP gene, 21 days after the transduction. The same field of cells was visualised with bright field (left column) and UV light (right column) in order to detect GFP expression. Various levels of GFP expression were observed in all cell lines, indicating successful and stable integration of the lentiviral genome.

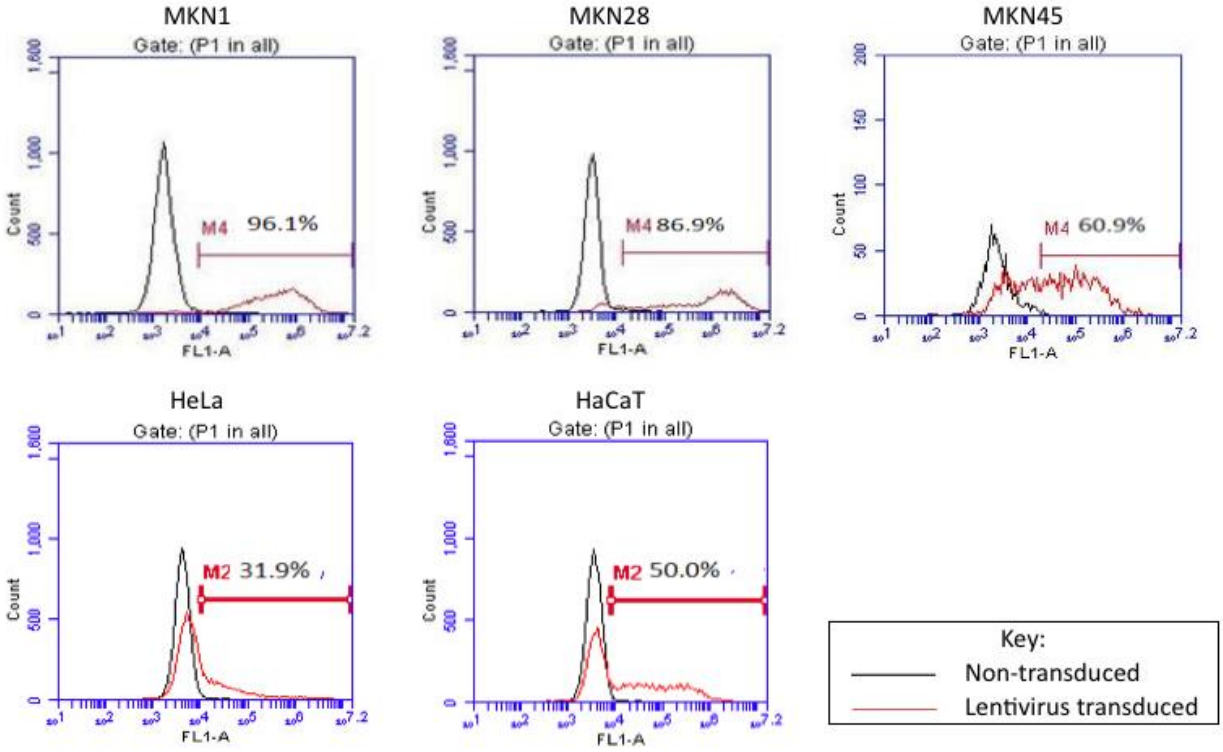

Figure 3.1.2 Analysis of GFP expression in lentiviral transduced epithelial cell lines
Flow cytometry analysis of non-transduced (black line) and lentivirus transduced (red line) cell lines (MKN1, MKN28, MKN45, Hela and HaCaT) was used to quantify the populations of cells expressing GFP (M4/M2 set at FL1>99% of non-transduced cells; value provided as a percentage in each panel). Intact cells were analysed by gating on this population using forward scatter and side scatter (not shown).Transduction efficiency ranged from 96.1% (MKN1) to 31.9% (HeLa).

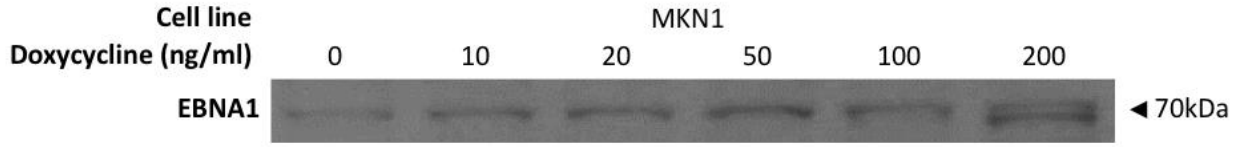

Figure 3.1.3 Assessment of inducible EBNA1 expression in lentiviral transduced MKN1 cell line

Western blot analysis of EBNA1 expression levels in the lentivirus transduced MKN1 cell line. Cells were treated with doxycycline (titrated between 0-200ng/ml) for 72h to induce the expression of EBNA1 (lentivirus incorporated gene) before harvesting. The protein levels were standardised and EBNA1 levels were assessed by western blotting. The inducible gene was seen to express low levels of EBNA1 in the absence of doxycycline, whilst treatment with high doses of doxycycline only slightly upregulated EBNA1 expression.

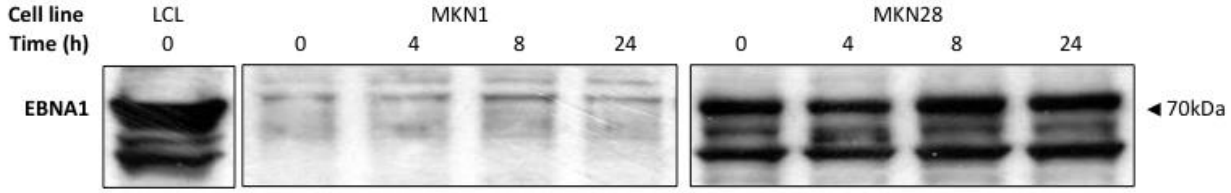

Figure 3.1.4 Analysis of induced EBNA1 stability in lentivirus transduced epithelial cell lines

Lentivirus transduced cell lines (MKN1 and MKN28) were treated with doxycycline (200ng/ml) for 48h, to induce the expression of EBNA1. The protein synthesis was then inhibited using cycloheximide (50µg/ml) and cells were chased for 0, 4, 8 and 24h. The protein levels were standardised and EBNA1 levels were assessed by western blotting. No changes in EBNA1 levels were observed across the 24 hours, indicating high levels of stability in both of the gastric carcinoma cell lines. *Note that all samples were analysed on the same blot.*

3.1.2 Transient transfection of epithelial cells with EBNA1

Rather than pursuing the lentiviral system in which inefficient levels of inducible EBNA1 were expressed by the transduced epithelial cell lines, I decided to use an alternative system utilising transient transfections to explore the key question of EBNA1 stability. Two reagents, Lipofectamine 2000 (Lipofectamine) and Mirus Transit X2 (Mirus), were compared in order to determine which was most appropriate for the transfection of a range of epithelial cell lines (MKN1, MKN28, MKN45, NUGC4, HeLa, 293FT and HaCaT). Both reagents were used in accordance with the manufacturer's protocol for the transfection of all cell lines with a plasmid encoding GFP expression (pCDNA3-GFP). Flow cytometry was used to quantify transfection efficiency (GFP expression) and cell viability (propidium iodide staining), comparing transfected cells to mock transfected control cells of the same type **(Figure 3.1.5)**. The cell viability for Lipofectamine transfected cells was consistently better than, or as good as the results from Mirus transfected cells. For transfection efficiency, the pattern varied between the two reagents depending on the cell line. However, the three fold increase seen for two gastric carcinoma cell lines, MKN1 and MKN45, was a significant factor in selecting the Lipofectamine reagent for use in all future transfections (Table S3.1.1 for data).

To find the optimal level of EBNA1 expression, different quantities (0, 2 or 4µg/ml) of pCDNA3-E1ΔGA were used for the transient transfection of the epithelial cell lines (MKN1, MKN28, MKN45, 293FT, HeLa and HaCaT). The transfected cells were harvested after 72h and EBNA1 levels were assessed using western blotting **(Figure 3.1.6)**. For all cell lines except HaCaT, the transfection using 4µg/ml DNA resulted in good levels of EBNA1 expression, surpassing physiological levels of EBNA1 seen in the LCL or MKN28 cell lines. Surprisingly low levels of EBNA1 were expressed in HaCaT cells, considering the levels of transfection efficiency that had been shown previously (comparable to the levels seen by the HeLa cell line). For all cell lines

apart from HaCaT, the EBNA1 expression levels roughly correlated with the previously determined transfection efficiencies; high levels for MKN28 and 293FT cell lines compared to lower levels in MKN1, MKN45 and Hela cell lines.

An EBNA1 stability assay was attempted to measure the natural degradation of EBNA1 over time. However, assessing the results of the stability assay was hindered by the technical limitation of low protein yields harvested from transfected cells treated with cycloheximide. After upscaling the experiment, data was generated for MKN1, MKN28, HeLa and MJS cell lines. The cell lines were transfected with pCDNA3-E1ΔGA (4µg/ml), allowing 48h for EBNA1 levels to accumulate. Protein synthesis was then inhibited by the addition of cycloheximide (50µg/ml) and cells were chased for 0, 4, 8 or 24h. The protein levels were standardised and the levels of EBNA1 assessed using western blotting **(Figure 3.1.7)**. In all cell lines, the consistent band intensity shown across 24h, in comparison to the BIP loading control, demonstrated high levels of EBNA1 stability within the epithelial cells. In contrast, the short lived protein cyclin D2 shows rapid degradation, with a half-life of <4h after treatment with cycloheximide.

Following on from these results, it was important to assess whether the epithelial cell lines possessed functional autophagy pathways. As the Tellam *et al.* study demonstrated that the rapid degradation of EBNA1 was unaffected by proteasome inhibition [47], this suggested an alternative mechanism for the low levels of stability observed. Autophagy could be a mechanism for this, as it is an important pathway for EBNA1 processing and presentation in B cells [25]. Therefore, the high levels of EBNA1 stability observed in the epithelial cell lines I was testing might be explained if the same cell lines were found to lack functional autophagy pathways. The levels of autophagy were measured using the gold standard method of a LC3 flux [56], which compares levels of LC3-II from cells cultured either in the presence or absence of a lysosomal

inhibitor (bafilomycin A1). The LC3 flux was performed in cell lines (MKN1, MKN28, Hela, HaCaT and MJS) under normal culturing conditions (10% FCS) and serum starvation (0% FCS), which is known to increase autophagy, for 6h. The LC3-II levels were assessed using western blotting **(Figure 3.1.8)**. This analysis demonstrated that the HeLa, MKN1 and MKN28 cell lines have high levels of basal autophagy, which can be upregulated by serum starvation. The results also showed that the LC3-II level in the HaCaT cell line was low, but autophagy is active both basally and under serum starvation. The exception here was the MJS cell line, which showed no basal autophagy; autophagy could however be upregulated upon serum starvation. By relating these results to the previous experiment, it was apparent that a lack of basal autophagy was not responsible for the EBNA1 stability within these epithelial cell lines.

As the nuclear location of EBNA1 protects it from autophagic degradation [45], in theory a cytoplasmic-EBNA1 variant may not be granted the same protection and might therefore have lower levels of endogenous stability in cells that have high autophagy levels. To assess if the high basal levels of autophagy within the epithelial cells would affect the endogenous stability of cytoplasmic-EBNA1, cell lines (HeLa and MKN28) were transfected with pCDNA3-E1ΔNLk/o (4µg/ml) and cultured for 48h to allow EBNA1 levels to build up. Protein synthesis was then inhibited with the addition of cycloheximide (50µg/ml) and cells were chased for 0,4,8 or 24h. The levels of EBNA1 were determined using western blotting **(Figure 3.1.9)**. Despite the high levels of autophagy within both cell lines, levels of cytoplasmic-EBNA1 (in comparison to the bip loading control) did not decrease over 24h. Unfortunately, two short life protein controls cyclin D2 and cyclin E were completely undetectable in cells treated with cycloheximide, although both were present for the LCL control.

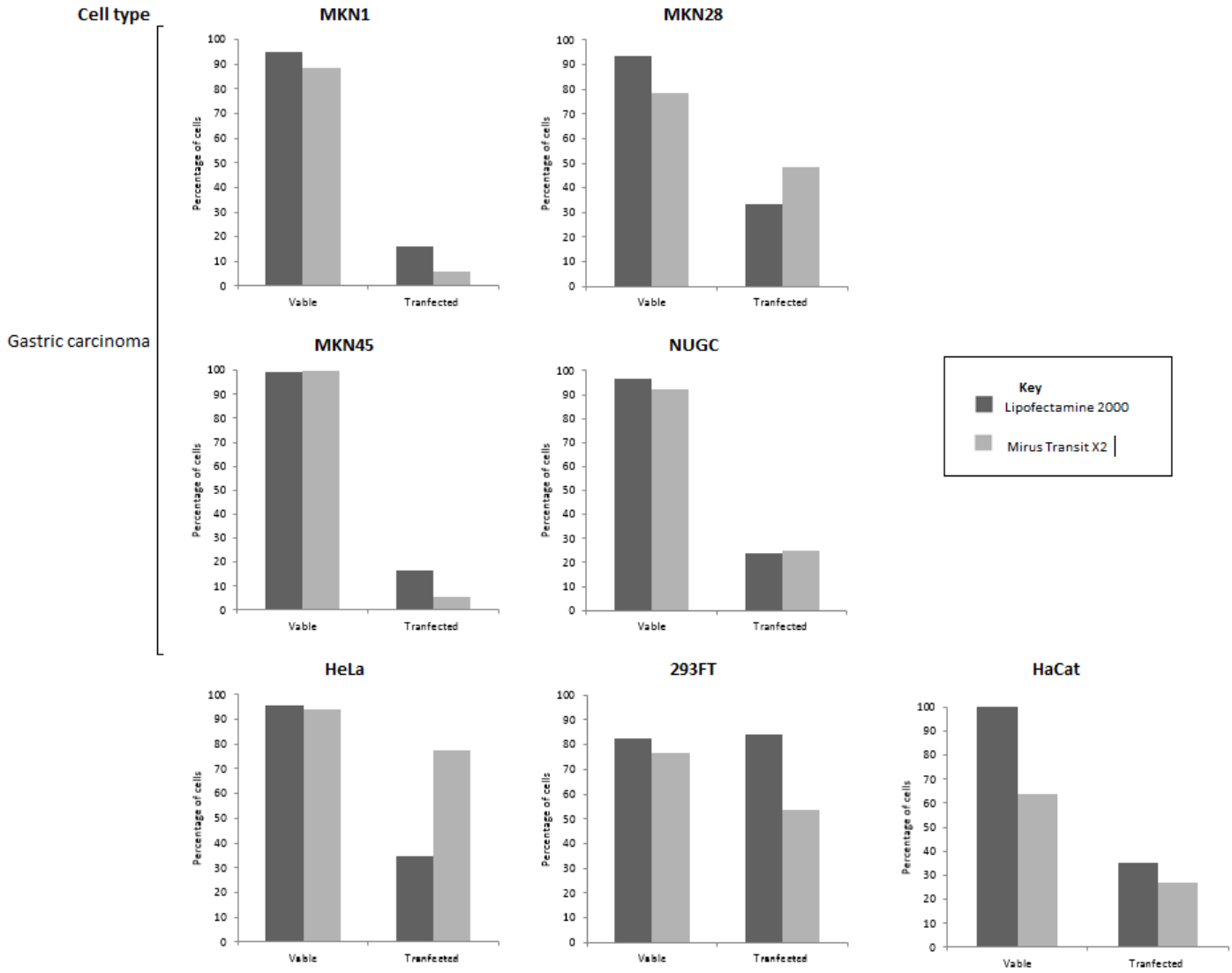

Figure 3.1.5 Comparison of transfection reagents for use on epithelial cell lines
The reagents Lipofectamine 2000 or Mirus Transit X2 were used to transfect the cell lines (MKN1, MKN28, MKN45, NUGC4, HeLa, 293FT and HaCaT) with 4µg/ml pCDNA3-GFP. Flow cytometry was used to assess transfection efficiency (GFP expression) and cell viability (propidium iodide staining), using mock transfected cells as a baseline reference point (Table S3.1 for values). Intact cells were analysed by gating on this population using forward scatter and side scatter (not shown). The results demonstrate that the cell viability was generally high (between 80-100%) for both reagents, but Lipofectamine transfections were consistently better, or as good as Muris transfection. The efficiency of transfections varied between the two reagents depending on the cell line; significantly however, a three-fold increase was seen for two gastric carcinoma cell lines, MKN1 and MKN45.

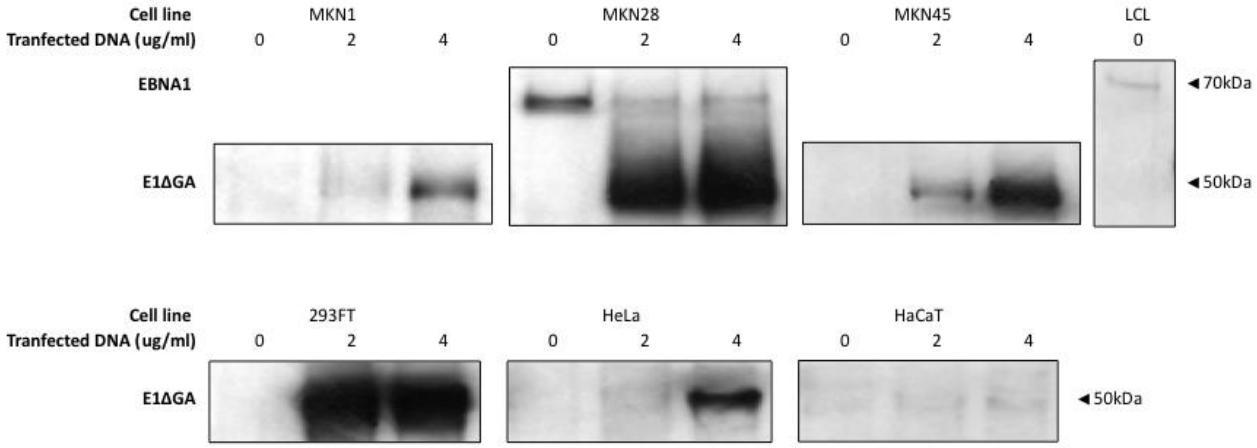

Figure 3.1.6 Optimisation of DNA concentration for the transfection of epithelial cell lines
Western blot analysis of EBNA1 protein levels in cells (MKN1, MKN28, MKN45, 293FT, HeLa and HaCaT). The cells were transfected with pCDNA3-E1ΔGA (0, 2 or 4ng/ml) and cultured for 48h before harvesting. Protein levels were standardised and EBNA1 levels were assessed by western blotting. Supraphysiological levels of E1ΔGA expression were seen from 4ng/ml transfections in all cell lines except HaCaT. An LCL was used as a positive control to indicate physiological levels of EBNA1 and mock transfected cells (0µg/ml) served as negative control for each cell line (illustrating the specificity of the antibody 1H-4). *Note that MKN1, MKN28, MKN45 and LCL samples were run and developed on the same blot. A second blot was used to run and develop all 293FT, HeLa and HaCaT samples.*

A)

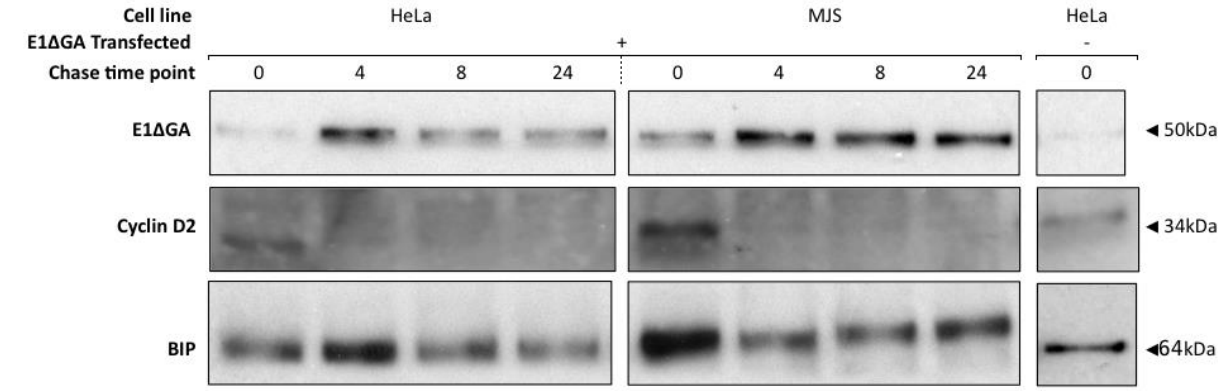

B)

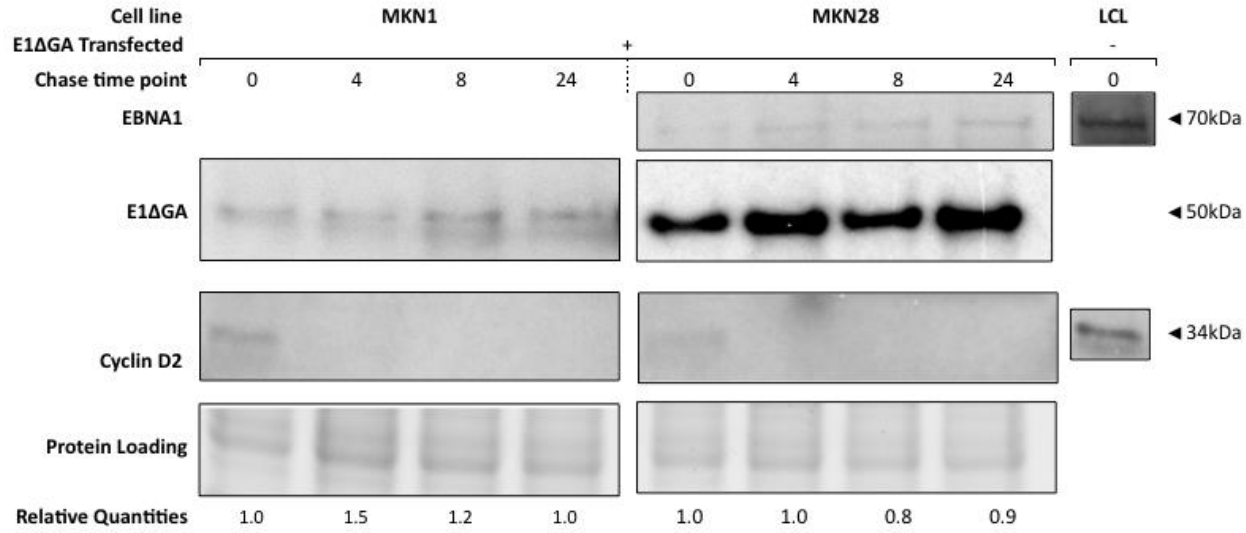

Figure 3.1.7 Analysis of E1ΔGA stability in transfected MJS and epithelial cell lines
A and B) The epithelial cell lines (HeLa, MKN1 and MKN28) and MJS were transfected with pCDNA3-E1ΔGA (4ng/ml) and cultured for 48h. Protein synthesis was then inhibited with the addition of cycloheximide (50µg/ml) and cells were chased for 0, 4, 8 or 24h. Samples were standardised and EBNA1 levels were assessed using western blotting. The consistent band intensity shown across 24h demonstrates that EBNA1 levels were stable in comparison to the loading controls for all cell lines. The blot was probed for Cyclin D2, serving as a positive control for a short lived protein, as seen by the rapid decrease in band intensity after 4h for all cell lines. A) Protein loading was assessed by probing the blot for BIP. B) Protein loading was assessed using ChemiDoc analysis of gel. *Note that HeLa and MJS and LCL samples were run and developed on the same blot. A second blot was used to run and develop all MKN1 and MKN28 samples.*

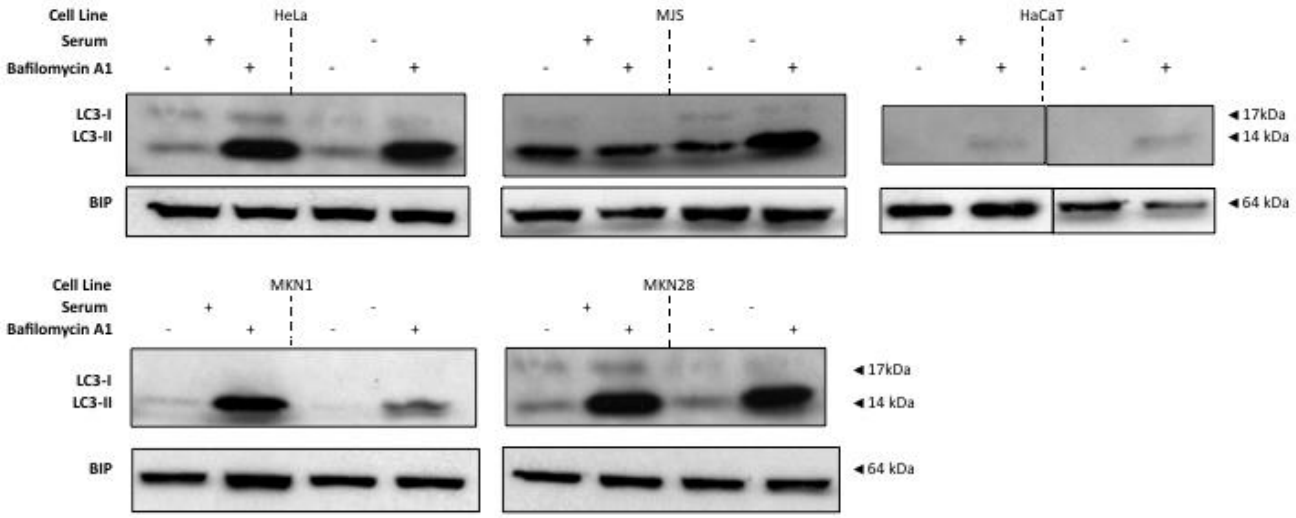

Figure 3.1.8 Analysis of autophagy (LC3) flux in MJS and epithelial cell lines
Epithelial cell lines (HeLa, HaCaT, MKN1 and MKN28) and MJS were cultured for 6h under normal culturing conditions (serum +) and under starvation (serum -), either with treatment of bafilomycin A1 (100nM), an inhibitor of lysosomal acidification, or untreated. The cells were harvested and standardised before determining LC3-II levels using western blotting. With the exception of MJS, all cell lines showed an increase in LC3-II band intensity with treatment of bafilomycin A1, indicating active levels of autophagy. This effect was increased further upon serum starvation. Whilst the LC3-II levels in HaCaT are low, autophagy is active both basally and under serum starvation. For MJS cells the LC3-II band intensity only increased from the addition of bafilomycin A1 when cells were serum starved. *Note that samples from HaCaT (serum +) and all samples from HeLa and MJS were run and developed on the same blot. A second blot was used to run and develop HaCaT (serum -) and all MKN1 and MKN28 samples.*

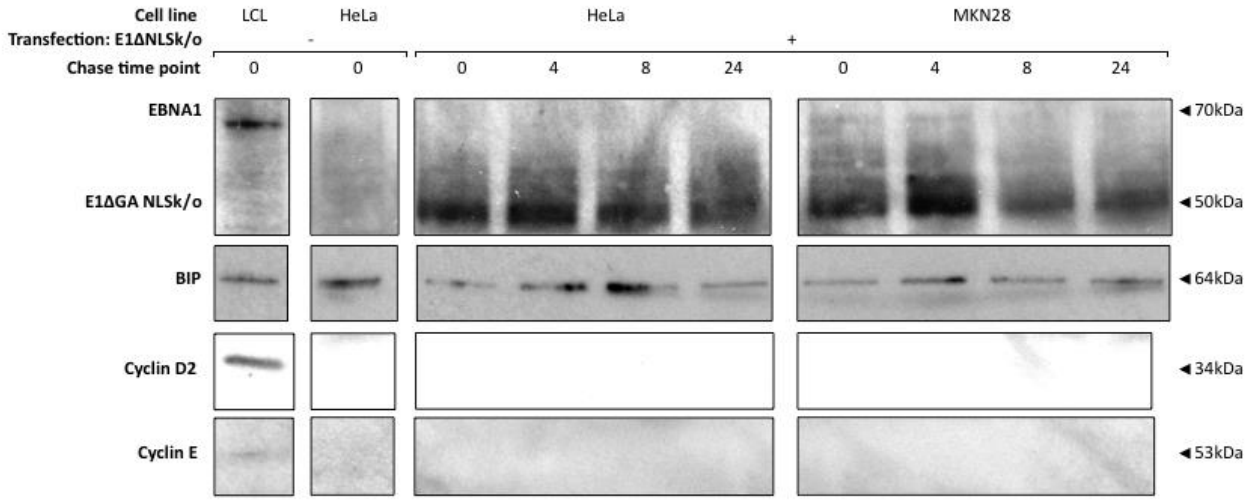

Figure 3.1.9 Analysis of E1ΔNLSk/o stability in transfected epithelial cell lines
Cell lines (HeLa and MKN28) were transfected with pCDNA3-E1ΔNLk/o (4ng/ml) and cultured for 48h. Protein synthesis was then inhibited with the addition of cycloheximide (50µg/ml) and EBNA1 was chased for 0, 4, 8 or 24h. The samples were standardised and EBNA1 levels were assessed using western blotting. The consistent band intensity, in comparison to the BIP loading control, shown across 24h demonstrates that E1ΔNLk/o is stable over 24h despite its cytoplasmic location. The blot was stripped and re-probed for short lived protein controls, cyclin D2 and cyclin E, but neither could be visualised for all the cells treated with cycloheximide. *Note that all samples were run and developed on the same blot.*

3.2 EBNA1 Presentation to CD4 T cells

3.2.1 EBNA1 specific CD4 T cell recognition of transfected epithelial cells

The previous results demonstrated that supraphysiological levels of both nuclear and cytoplasmic-EBNA1 were stable in epithelial cell lines, even in those possessing high levels of basal autophagy. Previous studies have illustrated that despite the stability of EBNA1 in B cells, there is still effective CD4 T cell recognition of MHC class II epitopes. The principle of effective CD4 T cell recognition relying on small quantities of processed protein may also apply to epithelial cells, where only small amounts of EBNA1 are degraded. I therefore conducted experiments to assess the ability of CD4 T cells to recognise epithelial cells' presentation of different EBNA1 variants, each with different abilities to access the MHC class II processing pathway.

Before conducting CD4 T cell assays, the epithelial cell lines were assessed to determine if they were capable of presenting MHC class II. The cell lines (MKN1, MKN28, MKN45, HeLa, HaCaT and 293FT) were cultured with and without IFNγ (100ng/ml) for 72h and then stained with conjugated antibodies specific for MHC class I or II. Levels of MHC presentation were determined using flow cytometry **(Figure 3.2.1)**. The results demonstrated that without IFNγ, none of the epithelial cell lines presented MHC class II. However, with the exception of 293FT, all of the cell lines had MHC class II presentation induced by the addition of IFNγ. Furthermore, whilst most cell lines naturally expressed MHC class I in the absence of IFNγ, the MKN45 cell line did not express MHC class I even with the addition of IFNγ. The experiment was repeated for MKN45 and 293FT cell lines and these results were confirmed. The fact that some EBV-associated epithelial malignancies can lose MHC class I expression whilst retaining MHC class

II, in the presence of cytokines, highlights the potential value of CD4 T cell responses against EBNA1.

Previous work in the laboratory by Leung and colleagues had extensively characterised the ability of two EBNA1 specific CD4 T cells clones, SNP (DR51-restricted) and VYG (DR11-restricted), to recognise LCLs [45]. I utilised these T cells for my novel investigation into epithelial cells presenting EBNA1 epitopes. A series of preliminary T cell assays were performed to determine whether the epithelial cell lines were HLA-matched for these, or potentially other, T cell clones available in the laboratory. The cell lines (Hela, HaCaT, 293FT, MKN1, MKN28 and MKN45) were incubated with IFNγ for 72h, allowing for the upregulation of MHC class II. The cells were then peptide pulsed with each T cell clone's cognate peptide. A T cell assay was then performed and the level of IFNγ released by the T cells was measured using an ELISA **(Table 3.2.1)**. The only positive match to an EBNA1 T cell clone was MKN45 (DR51) (Table S3.2.1). Unfortunately, due to technical difficulties, the HaCaT and MKN45 cell lines could no longer be cultured, resulting in these cell lines, along with 293FT cells (which could not present MHC class II), not being used in the future CD4 T cell assays. Therefore, to assess CD4 T cell recognition of EBNA1 epitopes, all epithelial cell lines required a co-transfection with plasmid encoding EBNA1 and the appropriate HLA type (as well as treatment with IFNγ to induce expression of MHC class II) prior to each T cell assay. It is worth noting here that an MJS cell line, which was not present in this experiment but used in the following T cell assays, is different to the sub-line used in the previous experiments on EBNA1 stability. Importantly, this new MJS cell line was not matched to either HLA DR11 or DR51 and, conversely to the previous MJS line, possessed basal levels of autophagy demonstrated by LC3 flux assay (data not shown).

To determine the optimal levels of DNA to be co-transfected into cell lines for the most effective T cell recognition, various amounts of DNA (0.2, 0.6 or 2µg/ml) for both HLA (DR51) and EBNA1 (E1ΔNLSk/o) were used in a co-transfection of MJS and MKN28 cell lines **(Figure 3.2.2)**. The results demonstrate that the optimal levels of DNA were 2ng/ml for EBNA1 and 0.6µg/ml of HLA-type. Samples from this experiment were also run on a western blot probing for EBNA1. This allowed a comparison between the amount of DNA transfected into the cells and physiological levels.

As well as testing the abilities of different EBNA1 variants to access the MHC class II processing pathway, the CD4 T cell assays were also used to compare two different epitopes, one of which was autophagy independent (VYG) and the other autophagy dependent (SNP) in B cells. The epithelial cell lines (MKN1, MKN28, MJS, HeLa and HaCaT) were co-transfected using one of several EBNA1 constructs (E1ΔGA, E1ΔNLSk/o or IiE1Δ) and a plasmid encoding HLA class II (DR11 or DR51) and treated with IFNγ for 72h. The transfected cells were then used in a T cell assay with CD4 T cells (VYG or SNP). The IFNγ release from this assay was measured using an ELISA. With a few exceptions, the same pattern of VYG T cell recognition for the different EBNA1 constructs was seen across all epithelial cell lines **(Figure 3.2.3)**. The model cell lines HeLa and MJS followed the expected pattern of EBNA1 variant recognition; low levels for nuclear EBNA1 with increased levels for cytoplasmic and the highest for the one tagged with invariant chain. This was followed by the maximum response for the cells pulsed with cognate peptide. Surprisingly, both gastric carcinoma cell lines, MKN1 and MKN45, deviated from this pattern with respect to the cytoplasmic-EBNA1, which showed lower recognition than the nuclear variant. For SNP, the same pattern of T cell recognition of different EBNA1 constructs was consistent across all epithelial lines **(Figure 3.2.4)**. As expected, recognition of EBNA1 variants featured low levels of recognition for nuclear, increased for cytoplasmic and highest when

tagged with an invariant chain. However, transfected cells pulsed with the cognate peptide for SNP showed lower levels of recognition than IiE1Δ.The mechanism for this consistent pattern of results across multiple experiments was unclear, as peptide pulsing was clearly functional as shown by the results from the HLA matched LCL control response. It was also notable that the MJS cell line had much higher levels of SNP T cell recognition for cytoplasmic-EBNA1, including the ratio of this to IiE1Δ, in comparison to other epithelial cell lines

All epithelial cell lines were capable of presenting autophagy dependent and independent epitopes to CD4 T cells. With a few exceptions, the hierarchy of EBNA1 variants' access to the processing pathway, previously shown in LCLs, appears to also apply to epithelial cells. However, it is difficult to compare levels of presentation between the epithelial cell lines or even to an LCL, as each line has a different transfection efficiency and MHC class II presentation.

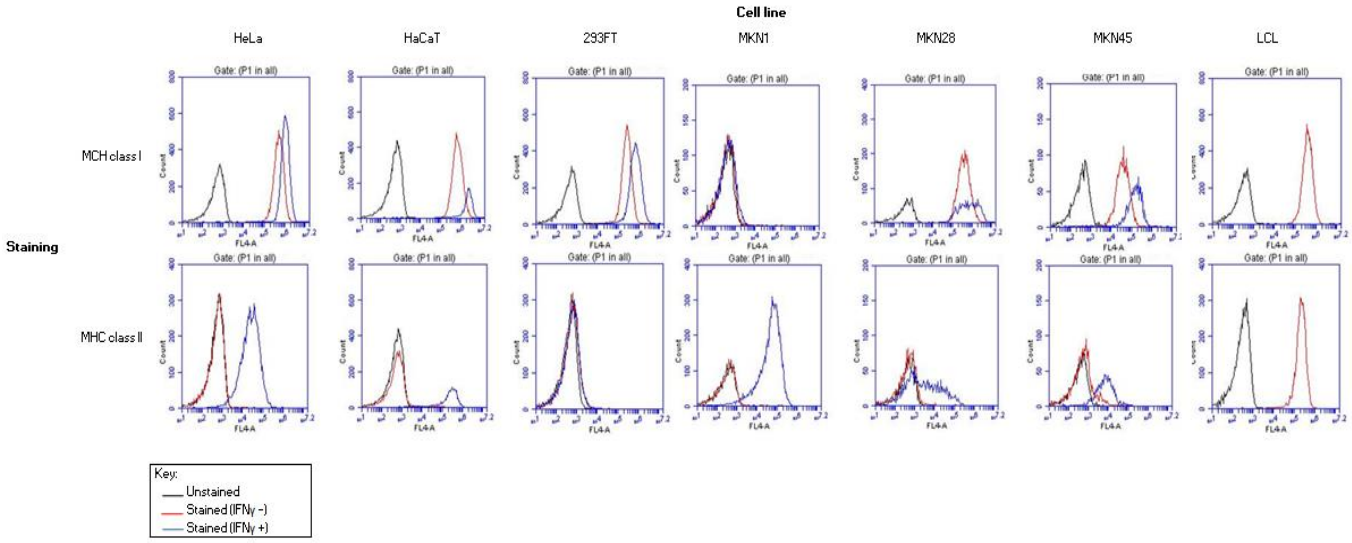

Figure 3.2.1 Analysis of MHC class I and II presentation for epithelial cell lines (+/- IFNγ)
Flow cytometry analysis of MHC class I and II surface presentation for epithelial cell lines (MKN1, MKN28, MKN45, HeLa, HaCaT and 293FT), cultured for 72h with or without the treatment of IFNγ (100ng/ml). The cells were then stained using conjugated antibodies APC-antihuman HLA-A,B,C and HLA-DR for the detection of MHC class I and II respectively (FL4 channel). Intact cells were analysed by gating on this population using forward scatter and side scatter (not shown). The MHC surface presentation was compared between unstained cells (black line), stained cells of the same line that had not been treated with IFNγ (red line) and stained cells that had been treated with IFNγ (100nm/ml)(blue line). An LCL possessing high levels of MHC class I and II was used as a positive control. The analysis demonstrated that without IFNγ, none of the epithelial cell lines present MHC class II. However, for all cell lines, with the exception of 293FT, the addition of IFNγ was sufficient to induce MHC class II presentation. The results also demonstrated that MKN45 had completely lost MHC class I presentation even with the addition of IFNγ.

Cell type	HLA determined by T cell assay
293FT	A2 and B7
HeLa	DR1, DR52b and DQ5
HaCaT	DQ6
MKN1	DR52b
MKN45	DR51 and DR52b

Table 3.2.1 Analysis of epithelial cell lines HLA restriction by T cell assay
The cell lines (Hela, HaCaT, 293FT, MKN1, MKN28 and MKN45) were incubated with IFNγ for 72h to induce the expression of MHC class II. The cells were then peptide pulsed with each T cell clone's cognate peptide. A T cell assay was then performed and IFNγ release was measured using an ELISA. The only positive match to an EBNA1 T cell clone was MKN45 (DR51).

A.

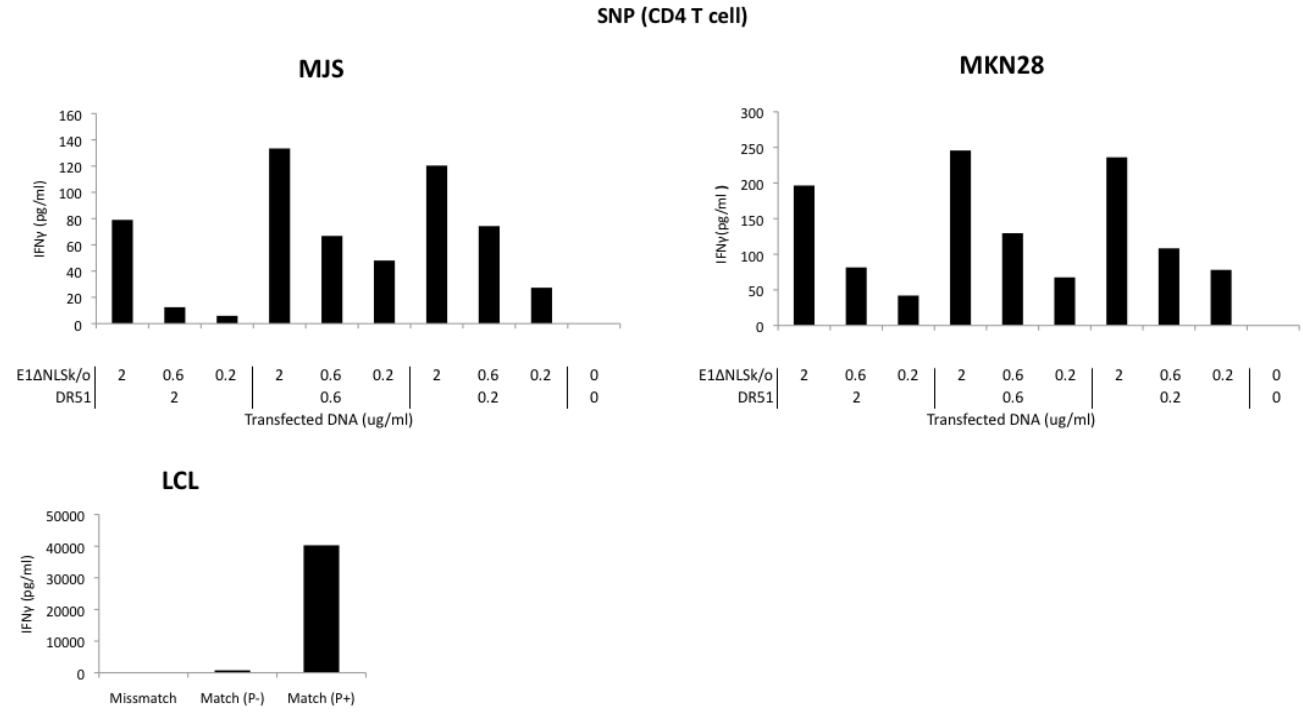

B.

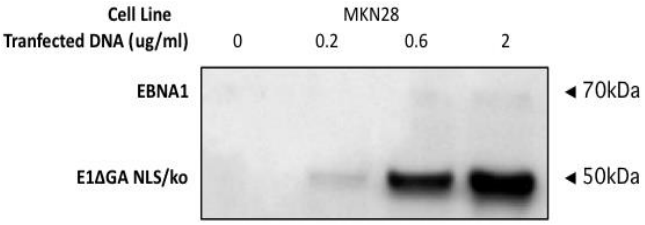

Figure 3.2.2 Optimisation of co-transfection for T cell assays for epithelial cell lines
A) ELISA analysis of IFNγ release assay from CD4 T cell, SNP, recognition of cell lines (MJS and HeLa) co-transfected with various concentrations of DNA plasmid (2, 0.6 or 0.2µg/ml) for the nine possible combinations of HLA (DR51) and EBNA1 (E1ΔNLSk/o). For all transfections, EBNA1 concentration was the limiting factor and the mid-level HLA concentration provided the optimal condition for T cell recognition. A HLA matched LCL was pulsed with the cognate peptide as a positive control, demonstrating T cell viability. B) Western blot analysis of E1ΔNLSk/o in MKN28 cells transfected with various concentrations of E1ΔNLSk/o. This blot demonstrated that the expression levels of transfected levels of DNA (even for the lowest concentration) were much higher than physiological levels of the full length EBNA1 naturally expressed in the MKN28 cell line.

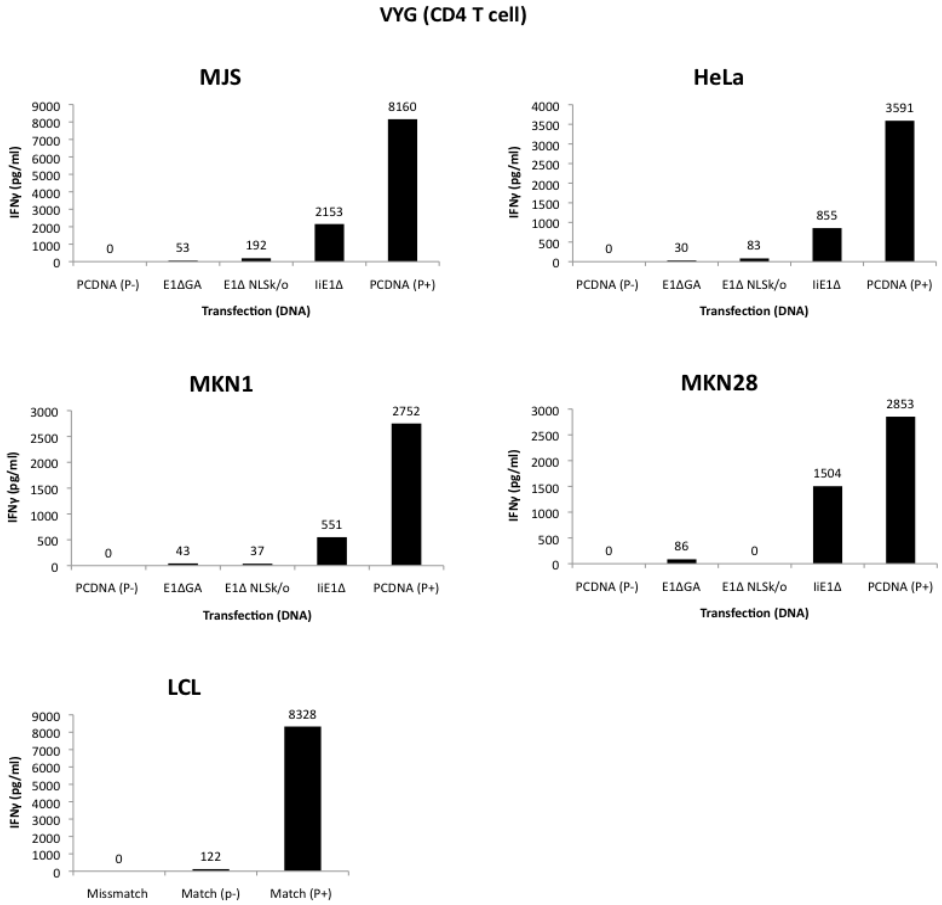

Figure 3.2.3 Analysis of VYG CD4 T cell assay with epithelial cell lines transfected with various EBNA1 constructs

ELISA analysis of IFNγ released from a T cell assay using a CD4 T cell clone (VYG) against target cell lines (MJS, HeLa, MKN1 and MKN28) co-transfected with a plasmid encoding HLA DR11 (0.6µg/ml) and a pCDNA3-EBNA1 plasmid (2µg/ml E1ΔGA, E1ΔNLSk/o or IiE1Δ) or an empty vector (pCDNA). The negative control, pCDNA (p-), was used as a benchmark (0pg/ml IFNγ). Physiological levels of T cell recognition against the endogenous EBNA1 protein present in MKN28 have therefore been subtracted to facilitate direct comparison of the various EBNA1 constructs. For the positive control, pCDNA (p+), some of the cells transfected with pCDNA3 were pulsed with synthetic VYG peptide to stimulate the maximum possible T cell response. With a few exceptions, the same pattern of VYG T cell recognition of EBNA1 constructs was observed across all epithelial lines over multiple experiments. The model cell lines, HeLa and MJS, followed the expected pattern of EBNA1 variant recognition; low levels for nuclear EBNA1, increased levels for cytoplasmic and highest for invariant chain. This was followed by the maximum response from the peptide pulsed cells. Surprisingly, both gastric carcinoma cell lines, MKN1 and MKN45, deviated from this pattern with respect to the cytoplasmic-EBNA1, which showed lower recognition than the nuclear variant. A HLA matched LCL was used as a positive control for the efficacy of the T cell, showing recognition of physiological levels of EBNA1 (p-) and maximum recognition after being peptide pulsed (p+).

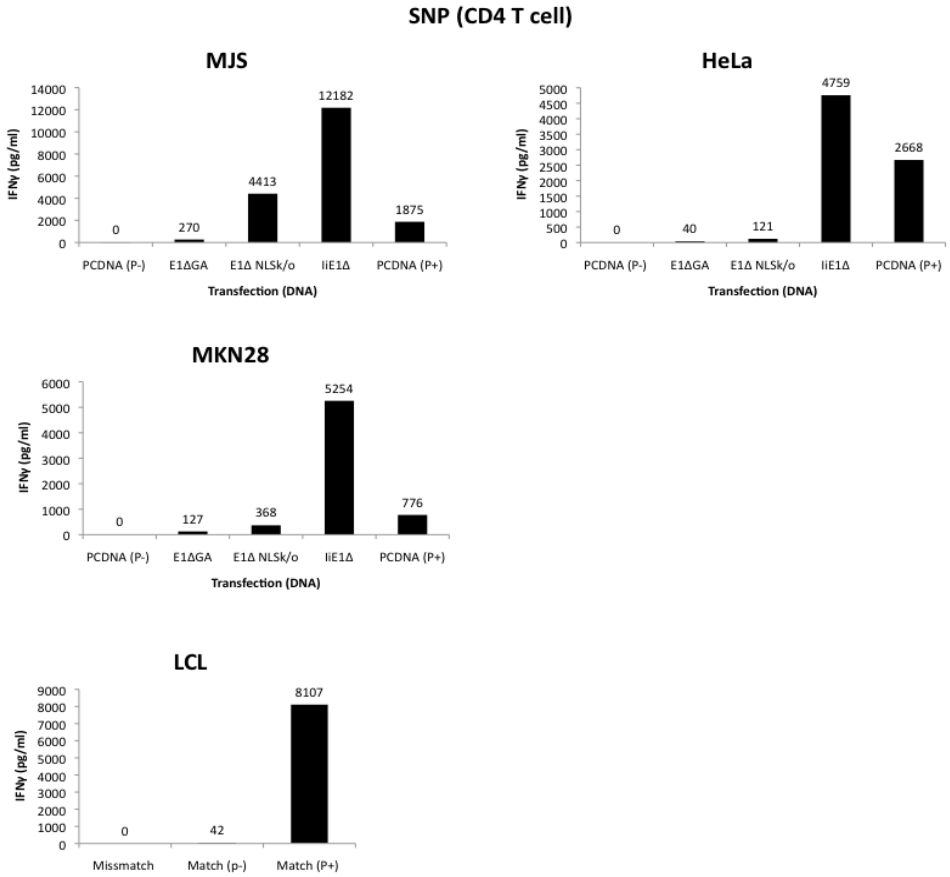

Figure 3.2.4 Analysis of SNP CD4 T cell assay with epithelial cell lines transfected with various EBNA1 constructs

ELISA analysis of IFNγ release T cell assay, using a CD4 T cell clone (SNP) against target cell lines (MJS, HeLa and MKN28) co-transfected with a plasmid encoding HLA DR51 (0.6µg/ml) and a pCDNA3-EBNA1 plasmid (2µg/ml E1ΔGA, E1ΔNLSk/o or IiE1Δ) or an empty vector (pCDNA). The negative control, pCDNA (p-), was used as a benchmark at (0pg/ml IFNγ). Physiological levels of T cell recognition against the endogenous EBNA1 protein present in MKN28 have therefore been subtracted to facilitate the direct comparison of the various EBNA1 constructs. For the positive control, pCDNA (p+), some of the cells transfected with pCDNA3 were pulsed with synthetic VYG peptide to stimulate maximum T cell response in the cell line. Recognition of EBNA1 variants followed the expected pattern; low levels of recognition for nuclear, increased levels for cytoplasmic and highest for invariant chain. Unexpectedly however, transfected cells pulsed with the cognate peptide for SNP then showed lower levels of recognition than IiE1Δ.The mechanism for this occurrence was unclear, as peptide pulsing was shown to be functional from the results of the HLA matched LCL (p+). It was also notable that the MJS cell line had much higher levels of SNP T cell recognition for cytoplasmic-EBNA1, including the ratio of this to IiE1Δ, in comparison to other epithelial cell lines. A HLA matched (DR51) LCL was used as a positive control for the efficacy of the T cell, showing recognition of physiological levels of EBNA1 (p-) and maximum recognition after being peptide pulsed (p+).

3.2.2 Effect of EBV-encoded miRNA on autophagy and CD4 T cell recognition

I next investigated the possible roles of miRNA in the processing and presentation of EBNA1. Data obtained by another laboratory suggested that the EBV-encoded miRNA BART 18 suppresses autophagy (E. Wiertz, University of Leiden, personal communication). If this is the case, then the expression of BART 18 may in turn affect the processing and presentation of certain autophagy dependent epitopes of EBNA1. In order to test this hypothesis, I received two cell lines from Wiertz's laboratory; an EBV-negative melanoma cell line (MJS) where miRNA was overexpressed and another EBV-positive Burkitt lymphoma B cell line (Jijoye) where miRNA was subject to knockout (k/o). The unmanipulated Jijoye cell line had previously been shown to express the BART 18 miRNA using m-R sensors. The Jijoye cell lines I received had been created using lentiviral transduction and positive selection to generate three sub-lines expressing different k/o miRNA plasmids: Empty vector (EV) k/o as a negative control, BART 16 (B16) k/o as an extra negative control (although it could theoretically be possible for this miRNA to have an unknown role that could affect either autophagy or antigen presentation) and BART 18 (B18) k/o. To test the effect of isolated B18 overexpression on autophagy levels and epitope presentation to CD4 T cells, an MJS cell line was selected as it possesses naturally high levels of MHC class II presentation and has previously been used as a model cell line for the study of antigen processing and presentation. The MJS cell lines I received had undergone lentiviral transduction and positive selection to generate four sub-lines overexpressing miRNA plasmids: EV overexpression, B16 overexpression, B18 overexpression and Cluster 1 (C1) overexpression (which contained BART 18-21). By experimenting with these two systems, loss of function and gain of function, BART 18 was assessed in terms of cellular autophagy levels and CD4 T cell recognition.

The autophagy levels in the MJS sub-lines overexpressing various miRNA vectors (EV, B16, B18 or C1) were assessed by performing an LC3 flux (previously described) **(Figure 3.2.5**). The data showed that all sub-lines had basal levels of autophagy under normal conditions, which were upregulated upon serum starvation. In terms of differences in autophagy levels between the miRNA constructs, the EV overexpression sub-line (negative control) showed much lower levels than the B16 overexpression (second negative control) sub-line. However, both these negative controls demonstrated lower levels of autophagy than the C1 and B18 overexpression sub-lines. This result appears to contradict the original hypothesis, as the individual expression of BART 18 caused an upregulation of autophagy levels rather than suppressing it.

The autophagy levels in the Jijoye sub-lines expressing various miRNA k/o vectors (EV, B16 or B18) were assessed by performing an LC3 flux (previously described), after which the levels of LC3-II were determined using western blotting **(Figure 3.2.6)**. Analysis showed that all cell lines had basal levels of autophagy under normal conditions, which was slightly increased upon serum starvation. Under normal conditions, the LC3-II band intensity increase was stronger in the EV k/o and B18 k/o sub-lines than in the B16 k/o sub line. Under starvation however, band intensity increase was strongest in the B18 k/o sub-line, with lower levels in EV and lower levels still in the B16 k/o sub-line. This result suggested that BART 18 only acted to downregulate autophagy in times of physiological stress, such as starvation (Table S3.2.2).

The effect of BART 18 on antigen presentation was then assessed in the various MJS and Jijoye sub-lines. Before performing T cell assays, it was important to measure the levels of MHC class II surface expression, as this might have impacted the levels of T cell recognition independently of the EBNA1 processing manipulated by miRNAs. All MJS and Jijoye sub-lines were cultured with IFNγ (100ng/ml) or left untreated for 72h. Staining with conjugated antibodies specific for

MHC class I or II then allowed assessment of MHC expression levels using flow cytometry **(Figure 3.2.7)**. The results here demonstrate that there was no variation for MHC class II presentation levels between the different sub-lines for either the MJS or the Jijoye cell line. Interestingly, there was a subtle variation in the MHC class I presentation between different sub-lines for both MJS and Jijoye cell lines. However, as I was not testing for CD8 T cell recognition this was not investigated further. The addition of IFNγ (10ng/ml) resulted in the upregulation of MHC class I and II equally for all MJS sub-lines, but had no impact on the Jijoye sub-lines; raising the concentration of IFNγ (100ng/ml) had no effect on these results (Figure S3.2.1).

I then investigated whether the processing of the different EBNA1 constructs, each with a capability of accessing the MHC class II processing pathway, was affected by the overexpression of BART 18. The MJS sub-lines overexpressing various miRNA vectors (EV, B16, B18 or C1) were co-transfected using an EBNA1 construct (E1ΔGA, E1ΔNLSk/o or IiE1Δ) and a plasmid encoding HLA class II (DR51) and cultured with IFNγ (10ng/ml) for 72h. The transfected cells were then used in an SNP CD4 T cell assay and IFNγ release was measured using an ELISA **(Figure 3.2.8)**. Equivalent levels of IFNγ production were seen in response in all sub-line variants, with a few exceptions. The C1 overexpression sub-line exhibited lower levels of recognition for E1ΔGA, IiE1Δ and peptide pulsed (P+). In the B18 overexpression sub-line the response to peptide pulsing was substantially higher than the other sub-lines. Finally, the C1 and EV overexpression sub-lines had lower responses for the nuclear EBNA1 in comparison to B18 and B16 overexpression sub-lines. There was therefore no discernible pattern for the overexpression of BART 18 alone effecting EBNA1 presentation.

To assess the effects of BART 18 loss of function on CD4 T cell recognition, the Jijoye sub-lines expressing various miRNAs k/o (EV, B16 or B18) were used to compare the autophagy

dependent epitope (SNP) against an autophagy independent epitope (VYG). As the EBV-positive Jijoye cell line was naturally MHC class II positive and HLA matched to both T cells (restricted though DR11 and DR51), it was used directly in a T cell assay and IFNγ release was measured using an ELISA **(Figure 3.2.9).** The B18 k/o sub-line showed a 0.5 fold increase in SNP T cell recognition compared to the two negative controls. For YVG T cell recognition the B18 k/o sub-line only showed a 0.2 fold increase from the two negative controls. Each cell line was pulsed with the cognate peptide of the T cell (SNP or VYG) as a positive control for maximum response. The SNP peptide pulsed cells showed consistent and strong recognition. However, a much weaker response was seen in VYG peptide pulsed cells, with a significantly lower value for the EV k/o sub-line. There appeared to be no obvious explanation for this.

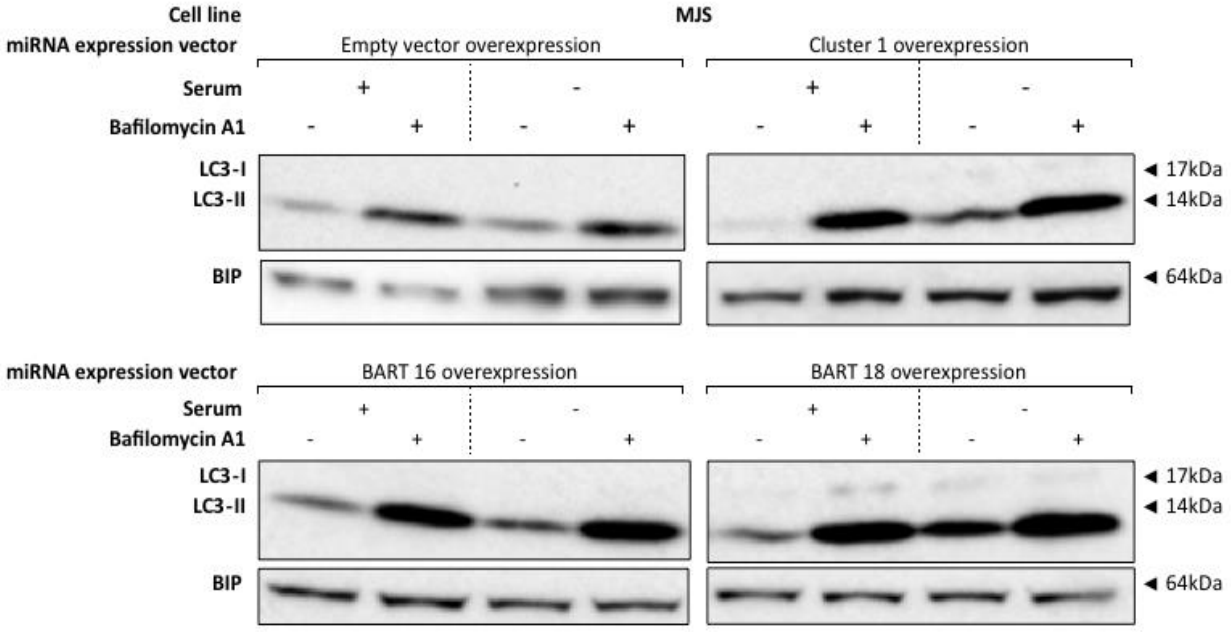

Figure 3.2.5 Analysis of autophagy (LC3) flux within various MJS sub-lines overexpressing miRNA vectors

Western blot analysis of LC3-II levels in various MJS sub-lines overexpressing miRNAs (Empty vector, Cluster 1, BART 16 and BART 18) cultured for 6h under normal culturing conditions (serum +) and under starvation (serum -), either with treatment of bafilomycin A1 (100nM), an inhibitor of lysosomal acidification, or untreated. The cells were harvested and standardised before determining LC3-II levels using western blotting. All sub-lines showed an increase in LC3-II band intensity upon inhibition of autophagy, indicating basal levels of autophagy. Band intensity increases were shown to be stronger for the C1 and B18 overexpression sub-lines compared to the EV and B16 overexpression sub-lines.

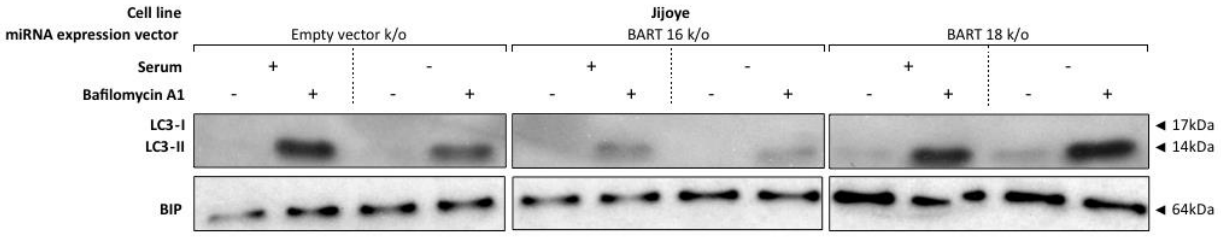

Figure 3.2.6 Analysis of autophagy (LC3) flux within various Jijoye sub-lines expressing miRNA k/o vectors

Western blot analysis of LC3 levels in various Jijoye sub-lines expressing miRNA k/o (Empty vector k/o, BART 16 k/o and BART 18 k/o) cultured for 6h under normal culturing conditions (serum +) and under starvation (serum -), either with treatment of bafilomycin A1 (100nM), an inhibitor of lysosomal acidification, or untreated. The cells were harvested and standardised before determining LC3-II levels using western blotting. All cell lines show basal levels of autophagy, with an increase in LC3 II band intensity upon autophagy inhibition. Under normal conditions, band intensity increases are seen to be stronger in the EV and B18 k/o sub-lines compared to the B16 k/o sub-line. Under starvation however, band intensity increase is strongest in the B18 k/o sub-line, with lower levels in the EV sub-line and lower levels still in the the B16 k/o sub-line.

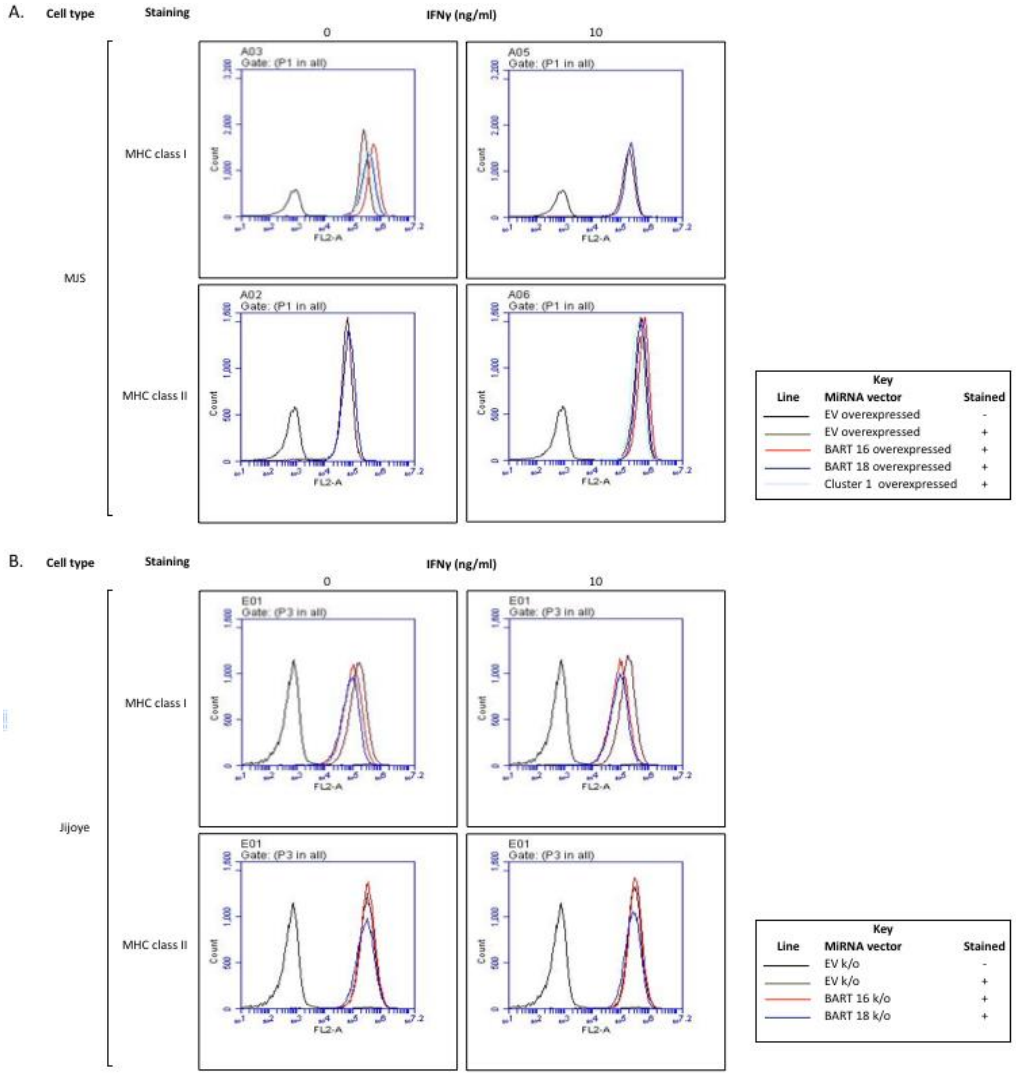

Figure 3.2.7 Analysis of MHC class I and II presentation of various Jijoye and MJS cell lines expressing miRNA constructs (+/- IFNγ)

Flow cytometry analysis of MHC class I and II surface presentation was assessed in all Jijoye and MJS sub-lines expressing the various miRNA vectors (overexpression and k/o). The cell sub-lines were left untreated (left column) or treated with IFNγ (10ng/ml)(right column) for 72h. The cells were then stained using MHC class I and II conjugated antibodies HLA-DR and HLA-A,B,C specific towards MHC class II and I respectively. Flow cytometry was used to measure fluorescence levels (FL2). Intact cells were analysed by gating on this population using forward scatter and side scatter (not shown). The MHC surface presentation was compared between unstained cells (black line) and stained cells (all other colours). Results show that both MJS and Jijoye cells are naturally MHC class I and II positive and the addition of IFNγ only causes upregulation in MJS cells. This result demonstrated that there was no difference in MHC class II surface presentation between the various miRNA sub-lines for either Jijoye or MJS. There was however a subtle variation in the MHC class I presentation between different sub-lines for both MJS and Jijoye cell lines

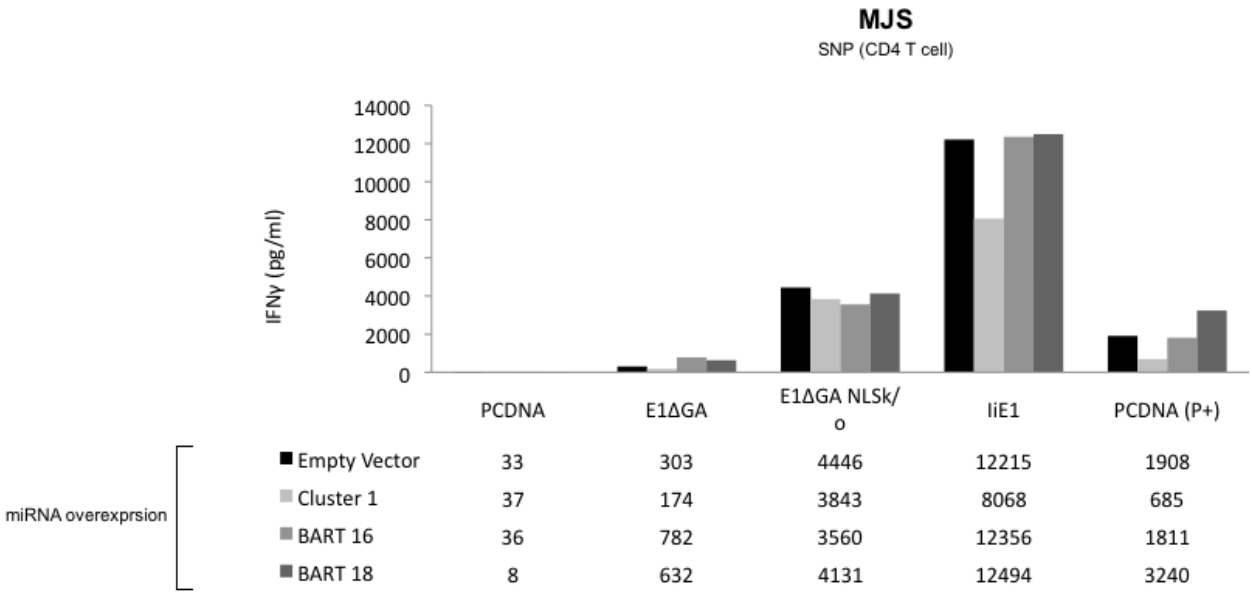

Figure 3.2.8 Analysis of SNP CD4 T cell assay with various MJS sub-lines, overexpressing different miRNA vectors, transfected with various EBNA1 constructs

ELISA analysis of IFNγ release from a T cell assay, using SNP T cell clones against target MJS sub-lines overexpressing miRNA (Empty vector, Cluster 1, BART 16 and BAR 18), co-transfected with plasmid encoding HLA-DR51 (0.6µg/ml) and an EBNA1 construct (2µg/ml), E1ΔGA, E1ΔNLSk/o or IiE1Δ, or pCDNA (2µg/ml). The results demonstrated similar levels of recognition between MJS sub-lines for each construct, with a few exceptions. The C1 overexpression sub-line exhibited lower levels of recognition for E1ΔGA, IiE1Δ and peptide pulsed (P+). In the B18 overexpression sub-line the response to peptide pulsing was substantially higher than in the other sub-lines. Finally, the C1 and EV overexpression sub-lines had lower responses for the nuclear EBNA1 in comparison to the B18 and B16 overexpression sub-lines.

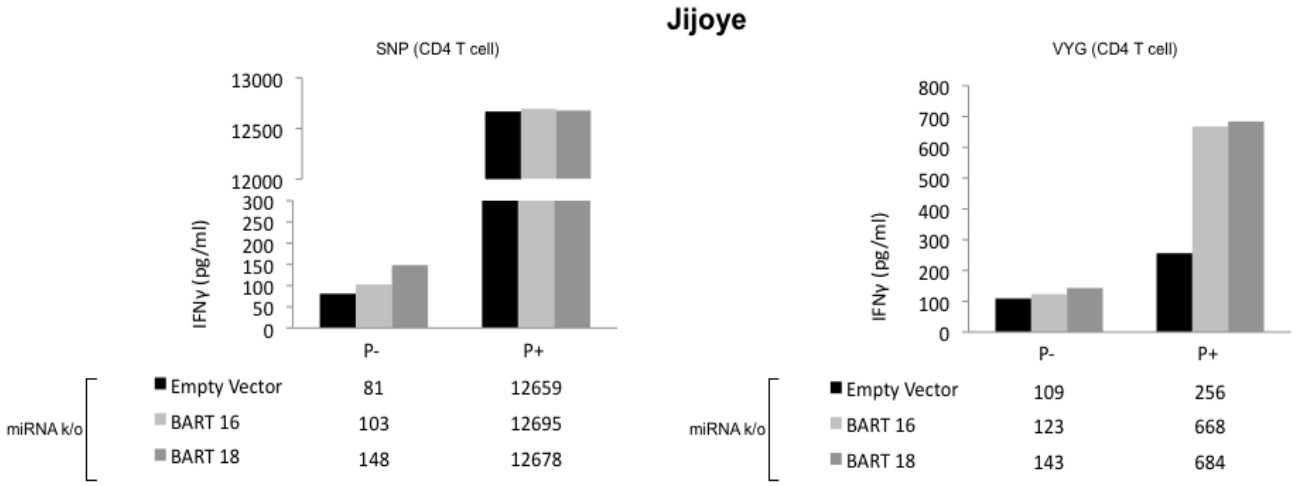

Figure 3.2.9 Analysis of SNP and VYG CD4 T cell assays with various Jijoye sub-lines expressing different miRNA k/o vectors

CD4 T cells, SNP or VYG, were incubated with the various Jijoye sub-lines expressing miRNA k/o vectors (Empty vector, BART 16 and BART 18), which had been peptide pulsed (P+) or left untreated (p-). The IFNγ release from the T cell assay was measured using an ELISA. For SNP recognition, the untreated B18 k/o sub-line showed a 0.5 fold increase in IFNγ levels compared to the two native controls, whilst the peptide pulsed cells for all sub-lines showed consistent recognition. Results from VYG demonstrated fairly even recognition across all miRNA variants. However, a very weak response was seen from the VYG peptide pulsed cells, especially from the EV k/o sub-line.

;

3.3 EBNA1 inhibition

Previous research has demonstrated that the inhibition of EBNA1 using dominant-negative inhibitors leads to an increase in MHC class I and MHC class II presentation of EBNA1 epitopes, which results in more effective T cell recognition [52]. Augmenting infected cells to improve T cell recognition may have applications in the immunotherapy of EBV-associated diseases. Until now, an investigation into whether pharmacological inhibitors of EBNA1 dimerisation have this same impact on T cell recognition has not been conducted.

3.3.1 Pharmacological inhibition of EBNA1 dimerisation for the manipulation of CD4 T cell recognition

Recently, an EBNA1 dimerisation inhibitor, JLP2, was designed using molecular computation [55]. The presence of the JL chromophore allowed the molecule to be visualised with confocal microscopy and quantified with flow cytometry. Upon treatment with JLP2, an EBV-positive NPC cell line was selectively visualised and was found to have reduced viability compared to the EBV-negative HeLa line. The collaborating laboratory (G. Wong, Hong Kong Baptist University) provided me with both JLP1 and JLP2 peptides. By treating EBV-positive cell lines with JLP2, I explored the specific visualisation, the effects on cell viability and the effects on CD4 T cell recognition.

Firstly, the fluorescent inhibitors were tested to see if they could effectively be used for the visualisation of EBV-associated cancer cell lines. EBV-positive cell lines (SNU, MKN28 and LCL (GT)) expressing EBNA1 and EBV-negative cell lines (MKN1 and HeLa) were both treated with JLP1 or JLP2 (20μM) for 12h. The fluorescence intensity was then assessed using fluorescent microscopy **(Figure 3.3.1)**. For both JLP1 and JLP2 there appeared to be non-specific extracellular binding for all cell lines regardless of whether they were EBV-positive or negative.

Upon testing the peptide alone (i.e. with no cells present), there was artifactual fluorescence from JLP2, with intensity levels that appeared almost as strong as when on cells. JLP1 was not used in any of the future experiments, as I wished to further investigate the claims regarding the JLP2 emission spectrum shift upon binding to EBNA1 and its effect on cell viability.

To more accurately assess JLP2 binding to EBNA1, flow cytometry was used to quantify the levels of green fluorescence. EBV-positive B cells, LCLs (GT and GS), were compared to EBV-negative B cells (Akata and Awaia), both having been treated with JLP2 (0 and 20μM) for 72 hours. Fluorescence was then assessed using flow cytometry (FL1) (**Figure 3.3.2)**. The results demonstrated that there was no fluorescence intensity change for either of the EBV-negative B cell lines treated with JLP2. However, there was a small rise in FL1(H) median intensity for both EBV-positive LCLs treated with JLP2, more prominently seen in LCL (GT). The small, but observable increase in fluorescence intensity suggested that specific binding of JLP2 was only occurring in EBV-positive B cell lines. However, a lower dose of JLP2 (5μM) was not sufficient to induce the increase in fluorescence for either EBV-positive LCL (data not shown).

Next, I was interested in replicating the previously published results showing JLP2's selective effect on reducing the viability of EBV-positive cell lines; in this previous model a comparison was made between C666.1 (EBV-positive NPC) and HeLa (EBV-negative epithelial) cell lines [55]. As these cell lines were from two completely different backgrounds, they were likely to behave differently in many ways. Therefore, for my experiment I decided to compare EBV-positive and negative cells from a similar B cell background. To assess JLP2's effect on cell viability, a WST-1 assay was optimised to find the best duration and density of B cells **(Figure 3.3.3)**. The effect of JLP2 on B cell proliferation was measured in various cell lines, which were EBV-positive (LCL (GT) and LCL (GS)) and EBV-negative (Akata and Awaia). The cell lines

were treated with various concentrations of JLP2 (0, 1, 5, 10 or 20μM) and chased for 4, 24, 48 or 72h. A 1h WST-1 assay with $5x10^4$ cells was used to measure cell viability **(Figure 3.3.4)**. The results demonstrate that JLP2 had a dose dependent effect, lowering the cell viability for the EBV-positive LCL (GT) after 4 hours; this effect was however reduced after 24h and completely lost after 48h. The JLP2 treatment did not have this effect on the cell viability of the two EBV-negative lines, but also did not affect the other EBV-positive LCL (GS). This suggested that in susceptible cell lines, the effect of JLP2 was very immediate but also transitory.

Finally, CD4 T cell recognition of JLP2-treated cell lines was assessed. HLA matched LCLs, GT (DR51) and GS (DR11), were treated with various concentrations of JLP2 (0, 10 or 20μM) and used in a CD4 T cell assay with SNP (DR51) or VYG (DR11). The levels of IFNγ release were assessed using an ELISA (**Figure 3.3.5)**. For both epitopes, a very slight increase was seen upon treatment with JLP2, however the effect was not dose dependent. Therefore it can be concluded that JLP2 did not appear to have a significant effect on the antigen processing for the MHC class II presentation of EBNA1.

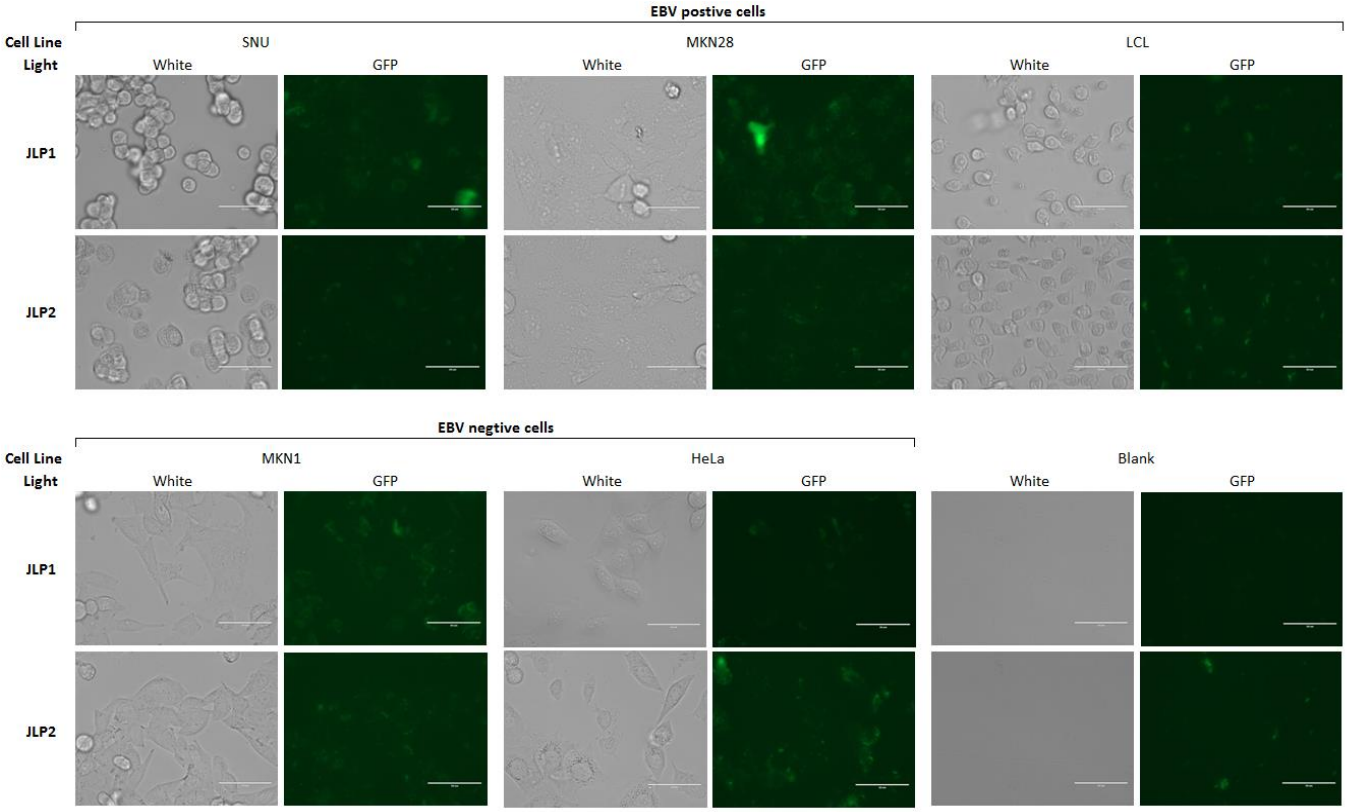

Figure 3.3.1 Visualisation of EBNA1 inhibitors, JLP1 and JLP2, treatment for various EBV-positive and negative cell lines

Fluorescence microscopy was used to visualise EBV-positive cell lines (SNU, MKN28 and LCL (GT)) and EBV-negative cell lines (MKN1 and HeLa) treated with either JLP1 or JLP2 (20µM) for 12h. The same field of cells was visualised under bright field and UV light to show the binding behaviour of JLP1 and JLP2. For both JLP1 and JLP2 there appeared to be non-specific binding for all cell lines regardless of EBV status. In the negative control, peptide alone with no cells (blank), there was no fluorescence of JLP1 but observable artifactual fluorescence of JLP2.

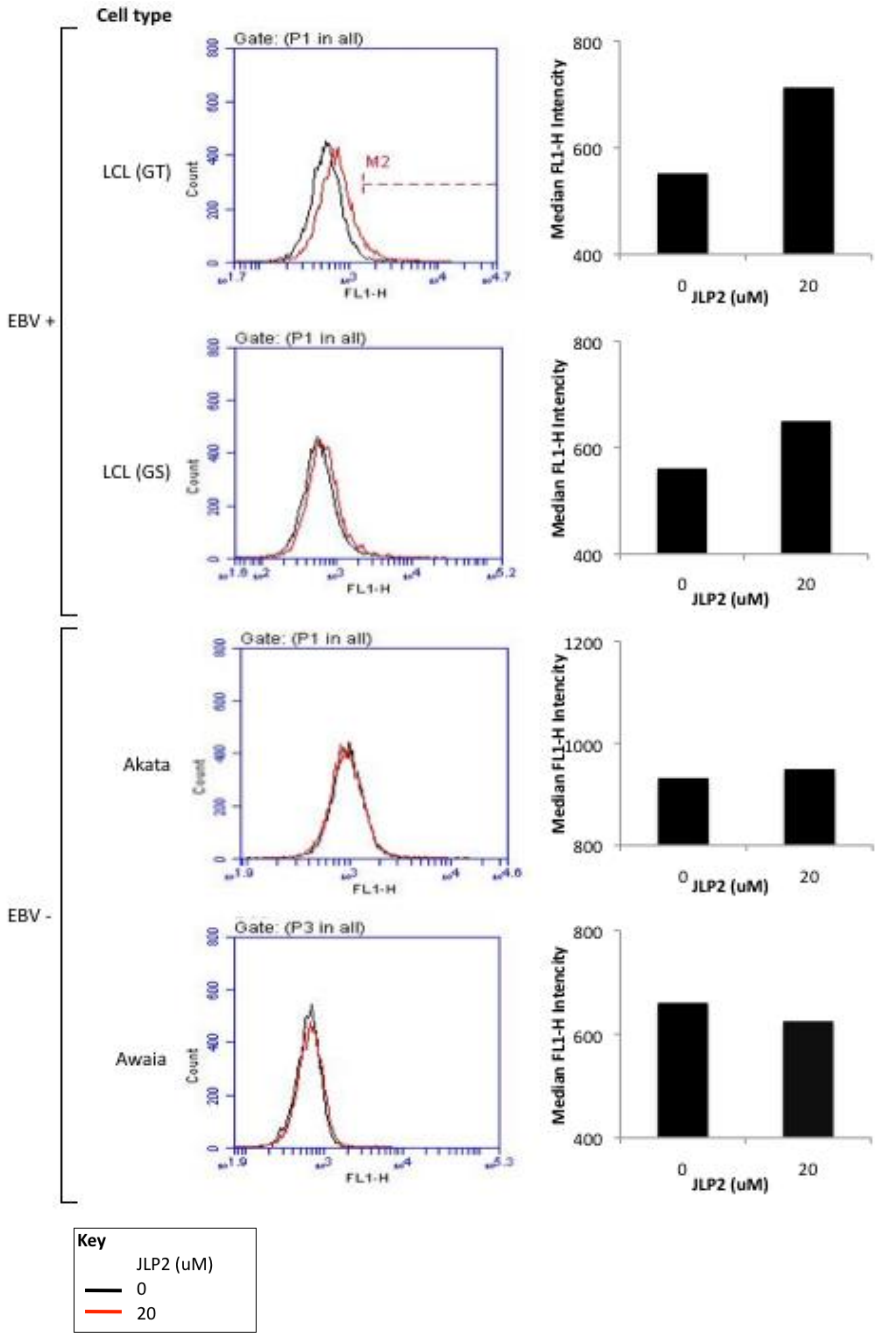

Figure 3.3.2 Analysis of JLP2 fluorescence in various EBV-positive and negative B cell lines

JLP2 fluorescence was assessed by flow cytometry in EBV-positive (LCL (GT) and LCL (GS)) and EBV-negative (Akata and Awaia) B cells, treated with JLP2 (0 or 20µM) for 72 hours. Intact cells were analysed by gating on this population using forward scatter and side scatter (not shown). The results showed a rise in FL1-H intensity for both EBV-positive LCLs treated with JLP2, more prominently seen in LCL (GT), which is not seen in the EBV-negative B cell lines. This shift verified specific binding of JLP2 in the EBV-positive B cell lines.

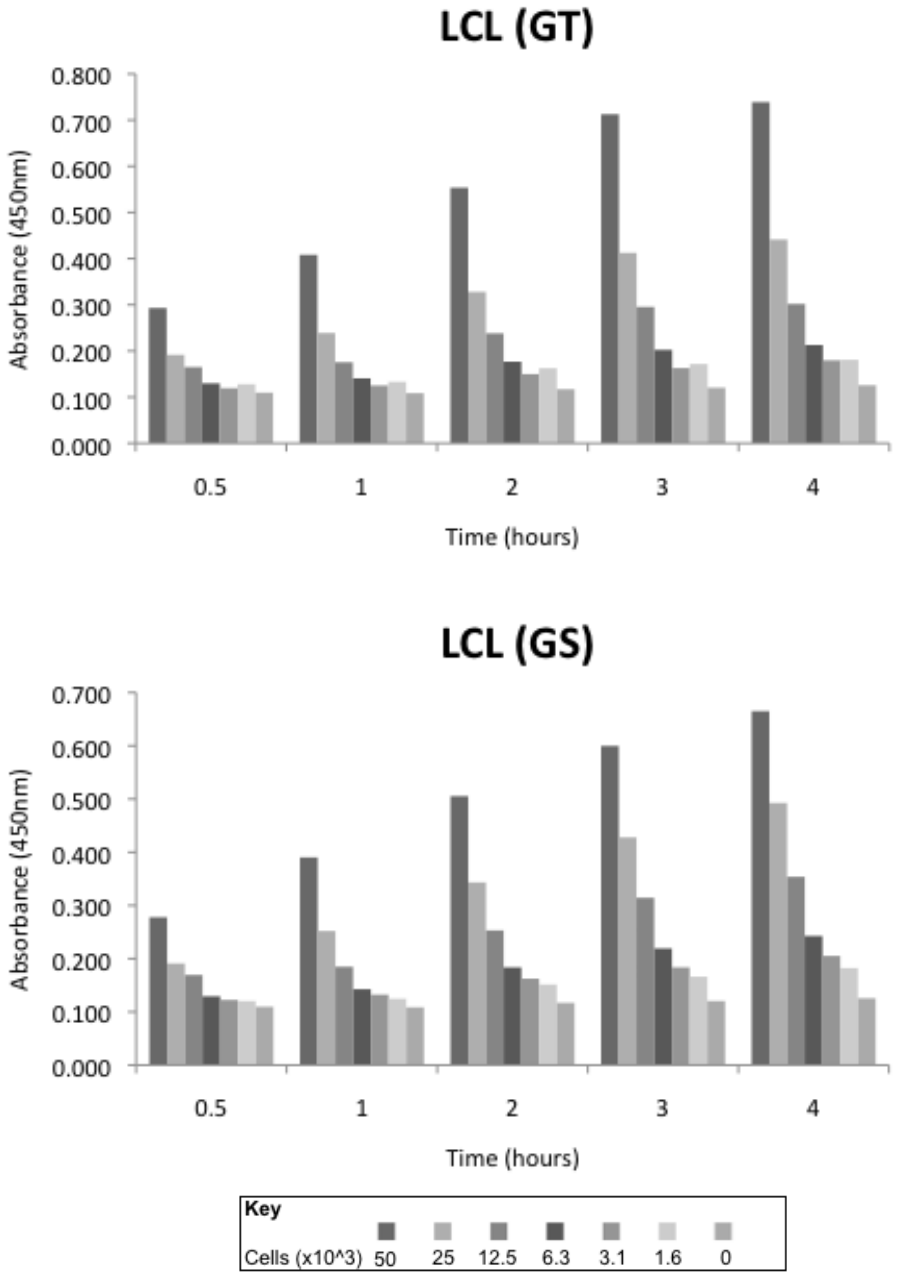

Figure 3.3.3 Optimisation for duration and B cell density for WST-1 proliferation assay
WST-1 proliferation assays were performed to find the optimal cell seeding density and time duration for use in future assays. WST-1 (10µl) was added to the LCL seeded at various densities (50, 25, 12.5, 6.3, 3.1, 1.6 or $0x10^3$). The samples absorbance (450nm) was measured at various time points over 4h (0.5, 1, 2, 3 or 4). The $5x10^4$ cell density incubated with WST-1 for 1h was used in future assays as it was most suitable for measuring cell proliferation and therefore cell viability.

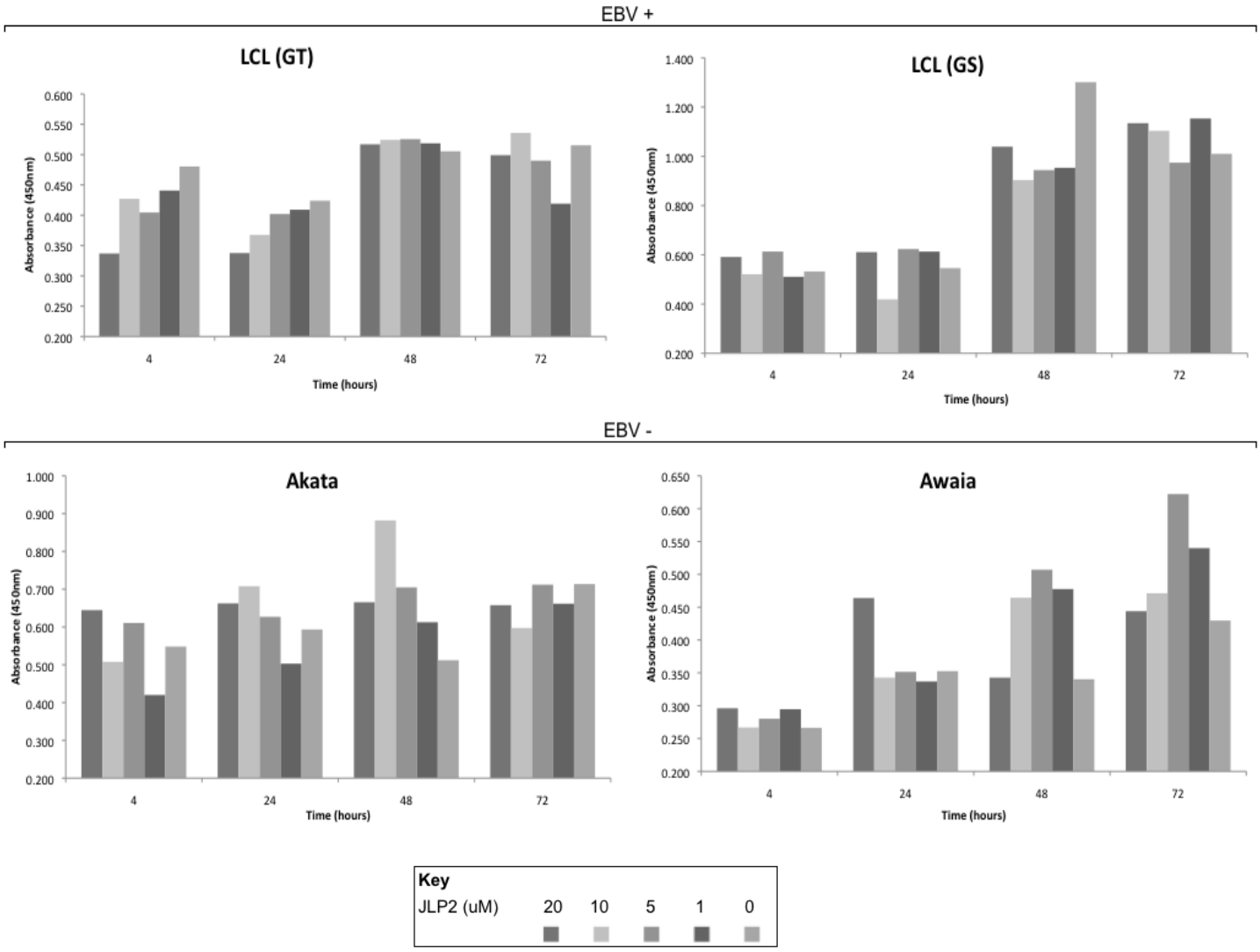

Figure 3.3.4 Analysis of JLP2 treatment's effect on the cell viability of various EBV-positive and negative B cell lines

EBV-positive (LCL (GT) and LCL (GS)) and EBV-negative (Akata and Awaia) B cells were treated with various concentrations of JLP2 (20, 10, 5, 1 or 0μM). The proportion of viable cells was determined at 4, 24, 48 or 72h after JLP2 treatment using a WST-1 assay. A JLP2 dose dependent effect on cell proliferation of LCL (GT) was observed after 4h, which reduced after 24h and was lost after 48h. The JLP2 treatment did not appear to have this effect on the two EBV-negative lines, but also didn't affect the other EBV-positive line, LCL (GS).

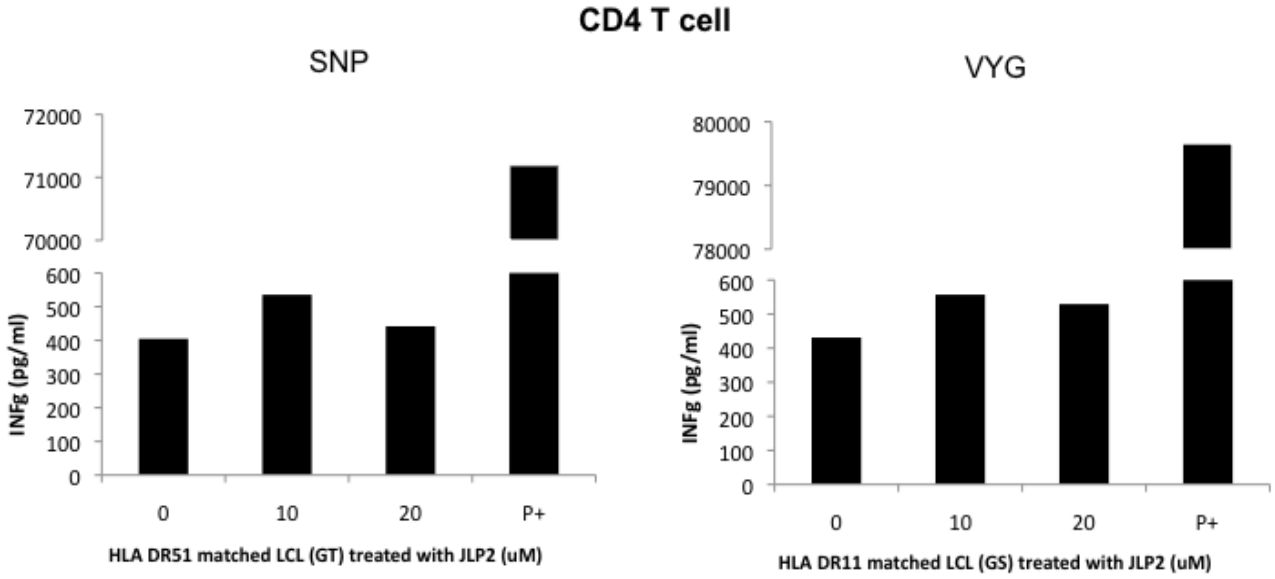

Figure 3.3.5 Analysis of VYG and SNP CD4 T cell recognition of EBV-positive LCLs treated with various concentrations of JLP2

HLA matched LCL targets for CD4 T cells SNP (DR51 - LCL (GT)) and VYG (DR11 - LCL (GS)) were treated with various concentrations of JLP2 (0,10 or 20µM) and used in a T cell assay. The IFNγ release was assessed using an ELISA. The results here demonstrated that for both epitopes a very slight increase was seen upon treatment with 10µM JLP2. This increase was sustained for VYG when the dose was increased to 20µM but not for SNP. Peptide pulsed (P+) LCLs were used as positive control and demonstrated the efficacy of the T cell clone. The IFNγ levels were standardised against a mismatched LCL T cell recognition (not shown).

4. Discussion

This work offers a novel perspective on EBNA1 processing and MHC class II presentation in the context of epithelial cancers. Over 200,000 malignancies each year are associated with EBV infections and the majority of these are found in epithelial cell backgrounds [42]. However, scientific research and clinical trials on the treatment of EBV-associated malignancies have almost exclusively focused on B cell lymphomas. The clinical relevance of utilising EBV targets for the treatment of EBV-associated diseases has been highlighted by the success of immunotherapies, such as adoptive T cell transfer for PTLD patients [33]. There is great potential to expand treatment options to cover the large number of patients with EBV-associated epithelial malignancies. Initial *in vitro* laboratory work studying relevant cell lines must be conducted first to elucidate the most appropriate effector T cell phenotype and EBV target for the treatment of these epithelial malignancies. In this study I investigated the CD4 T cell response to the EBV-encoded protein EBNA1 in the context of epithelial cells.

Within inflammatory tumour microenvironments, the presence of cytokines (such as IFNγ) can induce MHC class II presentation in many epithelial cell types, allowing for CD4 T cell recognition [57]. Moreover, cancer cells can be effectively controlled and even directly killed by CD4 T cells [16, 35]. The latent protein EBNA1, expressed within all EBV-associated malignancies, has a much wider range of epitopes for MHC class II compared to MHC class I. Thus, there is great potential in exploring whether EBNA1-specific CD4 T cells are effective at targeting and controlling EBV-associated malignancies. A study by Tellam and colleagues demonstrated that EBNA1 has a short half-life in an epithelial background compared to the long half-life observed in B cells [47]. Whilst this rapid degradation of EBNA1 within epithelial cells

was shown to be independent of proteasomal degradation, the mechanism for this degradation remains unclear and has not been explored further in the literature. One possibility is an autophagy dependent mechanism. If EBNA1 is susceptible to high levels of autophagic degradation in epithelial cells, more so than in B cells, this may contribute to more effective epitope presentation and greater levels of CD4 T cell recognition.

This project aimed to study EBNA1 stability and presentation to CD4 T cells in the context of epithelial malignancies. Furthermore, the claim that EBV-encoded miRNA BART 18 suppresses autophagy, potentially as a CD4 T cell recognition evasion strategy, was assessed. Tangentially, CD4 T cell recognition was also used to explore the possibility of using a pharmacological inhibitor of EBNA1 dimerisation to affect epitope processing and MHC class II presentation.

4.1 Endogenous stability of EBNA1

The results from Tellam *et al.* demonstrated that the endogenous stability of EBNA1 varied depending on cell type [47]. The expected long half-life (>30h) of EBNA1 expressed in B cells was shown, but a much shorter half-life was observed in the three epithelial lines tested. To expand on this work, I used several epithelial cell lines that were physiologically relevant to EBV-associated malignancies in which to study the endogenous stability of EBNA1.

4.1.1 The stability of EBNA1 in lentiviral transduced epithelial cell lines

Five epithelial cell lines were successfully transduced by an infectious lentivirus containing genes for an inducible full length EBNA1, as shown by the proportion of cells expressing GFP measured by flow cytometry. However, the inducible-EBNA1 gene could only be induced to low levels of expression, which did not reach the equivalent physiological level of EBNA1. The doxycycline (used for inducing gene expression) was independently validated by a separate experiment, where it induced the expression of a dox-regulated gene (data not shown). Because of the low level of EBNA1 expression, data from an EBNA1 stability assay was only generated in MKN1 and MKN28 cell lines. This experiment demonstrated that there was no apparent degradation of EBNA1 over the 24h chase, indicating high levels of stability (similar to the previously published results in B cells). As the MKN28 cell was naturally EBV-positive, stronger bands were seen in the western blot analysis due to the combination of physiological and induced EBNA1 expression. Technical challenges meant that this experiment lacked a loading control but the results suggest that EBNA1 levels remained mostly unchanged in these cell lines. Rather than attempting to fix the lentiviral system, I decided to focus on the key biological question of EBNA1 stability using a different experimental approach.

4.1.2 The stability of EBNA1 in transiently transfected epithelial cell lines

Optimisation experiments were performed to determine an appropriate transfection reagent and DNA concentration in order to generate supraphysiological expression of EBNA1 within the epithelial cell lines. Lipofectamine 2000 was selected as the transfection reagent, as it was three times more efficient in the transfection of two gastric carcinoma cell lines (MKN1 and MKN45) compared to the alternative transfection reagent Mirus Transit X2. The DNA concentration of 4µg/ml was chosen, as this demonstrated consistent supraphysiological expression of EBNA1 within all cell lines except HaCaT. Despite adequate transfection efficiency (35% shown by flow cytometry), only low levels of protein were seen for transfected HaCaT cells by western blot analysis. The HaCaT line was included in this study, as it was previously reported by Tellam *et al*. that EBNA1 had a very short half-life (<4h) in this cell background. However, I was only able to obtain a single preliminary result from the HaCaT cell lines (Figure S4.1.1), which suggested EBNA1 was stable with a long half-life in this cell background. Additional experiments in the HaCaT cell line would be needed to confirm this result.

To test the endogenous stability of EBNA1, the epithelial cell lines were transfected with a plasmid encoding E1ΔGA and a stability assay was conducted. I chose to use an E1ΔGA plasmid as it expresses higher levels of protein and Tellam *et al.* reported that there was no difference in the stability of full length EBNA1 compared to E1ΔGA expressed in either B cells or epithelial cells. The results from this stability assay demonstrated that for all tested cell lines, supraphysiological levels of E1ΔGA were stable and consistent in relation to the loading control BIP across the 24h chase, while a short-lived control protein was rapidly degraded in less than 4h. The data shown here is therefore inconsistent with the hypothesis of low EBNA1 stability levels in an epithelial cell background. However, as no mechanism explaining the short half-life of EBNA1 was given by Tellam *et al.,* other than showing that it was not proteasome dependent,

this still left the possible explanation of autophagy dependent degradation. Potentially, if the epithelial cell lines that I was using had no, or low, levels of basal autophagy compared to the epithelial cells used by Tellam *et al.*, this could explain the apparent stability of EBNA1 in my assays. However, upon measuring autophagy levels with an LC3 flux assay, all of the epithelial cell lines had high levels of basal autophagy under standard culturing conditions. The mechanism explaining the difference seen between my results and Tellam *et al.* was not discovered; potentially this could have been due to differences in the culturing, transduction or even variation between sub-lines of the same cell type. However, the principle of low stability of EBNA1 within epithelial cells is not supported by this data.

A cytoplasmic version of EBNA1 may be subject to higher levels of degradation, as the nuclear location of EBNA1 protects it from autophagic degradation [33]. However, upon testing gastric carcinoma cell lines (MKN1 and MKN28) transduced to express supraphysiological levels of E1ΔNLSk/o, the levels of cytoplasmic-EBNA1 did not decrease in comparison to the BIP loading control during a 24h stability assay. Although probing for two short lived protein controls was unsuccessful in both epithelial cell lines, all reagents used here had previously been tested and shown to work. Even with high levels of stability, only small amounts of protein degradation are required to generate robust T cell recognition.

4.2 CD4 T cell recognition of EBNA1 epitopes

4.2.1 EBNA1 specific CD4 T cell recognition of transfected epithelial cells

Despite the fact that EBNA1 appears stable within B cells, there is still enough endogenous processing to facilitate effective MHC class II presentation of EBNA1 epitopes to CD4 T cells. Although my previous work demonstrated that EBNA1 is stable within the epithelial cell lines, this does not discount the possibility of small levels of degradation providing enough MHC class II presentation for effective recognition by CD4 T cells. A study exploring the viral effects on antigen presentation in the melanoma cell line MJS (transfected with plasmids encoding for E1ΔNLSk/o and HLA-DR51) demonstrated that the expression of cytoplasmic-EBNA1 allowed for high levels of CD4 T cell recognition of the autophagy dependent epitope SNP [58]. To expand on this work, I designed systematic analyses measuring the recognition of different EBNA1 variants (each with different abilities to access the MHC class II processing pathway) in the context of epithelial cell lines and the MJS cell lines. Except for the 293FT cell line, all epithelial cell lines upregulated cell surface MHC class II levels in the presence of IFNγ. Whilst some of these expression levels were lower than the levels seen in B cells, they were high enough to elicit CD4 T cell recognition. By running a preliminary T cell assay, I discovered that none of the epithelial cell lines (that would go on to be used in future T cell assays) were HLA matched to the two EBNA1 CD4 T cell clones used (SNP-DR51 and VYG-DR11) in our laboratory. Therefore, all of the cell lines required co-transfection with an EBNA1 construct and a plasmid encoding an appropriate HLA-molecule, as well as treatment with IFNγ, prior to each T cell assay. Interestingly, the co-transfection optimisation to find an appropriate DNA concentration for T cell recognition demonstrated that while EBNA1 concentration was always the limiting factor for T cell recognition, increasing the concentration of HLA-encoding plasmid DNA to a high concentration (from 0.6 to 2μg/ml) consistently decreased T cell recognition for

both cell types tested. This is most likely due to the increased levels of toxicity from higher concentrations of DNA reducing cell viability [59], therefore leading to less transfected cells being present to stimulate T cells.

A CD4 T cell clone specific to the epitope VYG (an autophagy independent epitope from nuclear-localised EBNA1) was used to test the recognition of the epithelial and MJS cell lines, transfected with plasmids encoding different EBNA1 variants. The results showed that the recognition of these cell lines followed the same pattern as in LCLs (shown by a previous publication [45]); low levels of T cell recognition for the nuclear EBNA1 that increased for the cytoplasmic and was substantially higher for the invariant-chain variant. This was followed by the maximum possible stimulation of the T cell by the cell line that had been pulsed with the cognate peptide. While this pattern was followed by the HeLa and MJS cell lines, a notable exception was seen in both gastric carcinoma cell lines, MKN1 and MKN28, where the T cell recognition of cytoplasmic-EBNA1 was equal to or lower than recognition levels of the nuclear variant. In earlier protein stability assays both gastric carcinoma cell lines displayed very high levels of cytoplasmic-EBNA1 stability, which was indistinguishable from the stable nuclear EBNA1. It would therefore be interesting to compare the stability of cytoplasmic-EBNA1 in the other epithelial cell lines, with higher levels of cytoplasmic-EBNA1 recognition in future work.

A CD4 T cell clone specific to the epitope SNP (an autophagy dependent epitope from nuclear EBNA1) was used to test the recognition of the MJS and all but one of the epithelial cell lines, transfected with plasmids encoding different EBNA1 variants. Again, the results showed that the recognition of these cell lines followed the same pattern as in LCLs (shown by a previous publication (Leung)); low levels of T cell recognition for the nuclear EBNA1 that increased for the cytoplasmic and was substantially higher for the invariant-chain variant. However, the cells that

were pulsed with the cognate peptide for SNP did not exhibit the maximum recognition levels, as IFNγ levels were consistently lower than the response to the transfected IiE1Δ variant. The mechanism for this pattern, seen consistently across multiple experiments, was unclear. The cognate peptide itself was validated by the good levels of T cell recognition of the peptide pulsed HLA matched LCL control. Potentially, the transfected HLA-DR51 was capable of functioning correctly with the presentation of endogenous proteins, but for unknown reasons was not fully responsive to peptide pulsing. The data could also suggest that the endogenous antigen processing pathway is actually manipulating the final epitope, which resulted in greater levels of T cell stimulation compared to the pulsed peptide. This could possibly come from alterations being made to the variable peptide flanking residues (PFRs). PFRs extend from the N- and C-terminus of the MHC class II binding groove; whilst the core 9 amino acids remain unchanged, the PFR can be altered during the endogenous processing of antigens and there is evidence that this modulation will enhance CD4 T cell responses [60]. This phenomenon may therefore explain why the endogenously processed SNP peptide appears to give a stronger T cell response than the un-processed peptide used for pulsing cell. Another conceivable cause of this could have been an unknown factor affecting the cell lines used, although this seems unlikely as peptide pulsing worked in the same cell lines for the previous experiment with the transfected HLA-DR11. In this experiment it was also noticeable that the MJS cell line had much higher levels of SNP T cell recognition for cytoplasmic-EBNA1, including a ratio of cytoplasmic to invariant-chain IiE1Δ, in comparison to the epithelial cell lines. The mechanism of differential processing pathways of SNP and VYG from cytoplasmic-EBNA1 in the gastric carcinoma cell line was not explored further, but as it is different to B cells this could form the basis of future experiments regarding EBNA1 antigen processing and presentation.

4.2.2 The effect of EBV-encoded miRNA on autophagy and CD4 T cell recognition

Small non-coding RNA sequences, known as miRNAs, are able to regulate protein expression by binding to complementary sections of miRNA. In its latent phase, EBV expresses many miRNAs that affect the host cell's expression profile, including some that have oncogenic properties such as enhancing a cell's propensity for immortalisation [61]. Recent preliminary research has suggested that EBV-encoded miRNA, BART 18, contributes to suppressing autophagy within the host cells (E. Wiertz University of Leiden, personal communication). In theory, this would give a selective benefit to EBV by limiting the processing and therefore presentation of certain autophagy dependent epitopes of EBNA1 to CD4 T cells. To test this hypothesis, I collaborated with Wiertz's laboratory, which provided me with two cell lines; an EBV-negative melanoma cell line (MJS) and an EBV-positive Burkitt lymphoma cell line (Jijoye). The Jijoye cell line, which had previously been shown to express the BART 18 miRNA using m-R sensors, had been manipulated through lentiviral transduction and positive selection to generate three sub-lines expressing different plasmids that knocked out the function of particular miRNAs: Empty vector (EV) k/o as a negative control, BART 16 (B16) k/o as an extra negative control (although it could theoretically be possible for this miRNA to have an unknown role that could affect either autophagy or antigen presentation) and BART 18 (B18) k/o. As a complementary strategy an MJS cell line, which would be used to study the miRNA expression in isolation from the rest of the EBV genome, had been subjected to lentiviral transduction and positive selection to generate four sub-lines expressing different plasmids overexpressing miRNAs: EV overexpression, B16 overexpression, B18 overexpression and Cluster 1 (C1) overexpression (which contained BART 18-21). Within these two systems, loss of function and gain of function, I explored the effect of BART 18 on autophagy levels and CD4 T cell recognition.

The analysis of autophagy levels in the MJS sub-lines, overexpressing vectors (EV, B16, B18 or C1), demonstrated that all lines had basal levels of autophagy under normal conditions. However, both sub-lines overexpressing B18 (B18 and C1) had higher basal autophagy levels in comparison to the negative controls (EV and B16 overexpression sub-lines). With the overexpression of BART 18 resulting in increased autophagy levels, my data entirely contradicted the original hypothesis from the Wiertz laboratory.

The analysis of autophagy levels in the Jijoye cell lines, expressing various miRNA k/o vectors (EV, B16 or B18), demonstrated that all of the lines had basal levels of autophagy. Under normal conditions, low levels of autophagy were seen for the B16 k/o sub-line, while higher levels of autophagy were seen for the EV k/o and B18 k/o sub-lines, where the autophagy levels were equivalent. Again, this result did not support the original hypothesis. Interestingly upon serum starvation, the autophagy levels in the B18 k/o sub-line increased, whereas the autophagy levels in both the B16 k/o and EV k/o sub-lines (where B18 was still functionally expressed) were slightly reduced in comparison to the basal levels. This suggests that BART 18 only acts to downregulate autophagy in times of physiological stress, such as starvation. The data from the previous experiment, in which B18 was overexpressed in MJS cells, does not correlate with this result. It could however be possible that multiple factors are required to see this effect, implying that removing B18 affects the pathway but expressing it alone is not sufficient to trigger the mechanism. Multiple miRNAs can be required to co-regulate certain functions, a phenomenon known as miRNA synergy [62]. This hypothesis of BART 18 and unknown factors requires further investigation.

After documenting the effect of the miRNAs on autophagy levels, T cell recognition of the different sub-lines was explored. The MJS sub-lines (overexpression miRNAs) transfected with

the various EBNA1 constructs (discussed previously) were shown to have equivalent recognition of (autophagy dependent) epitope SNP from a CD4 T cell assay, with several exceptions. The key result was that no difference was observed in the B18 overexpression sub-line compared to the EV or B16 overexpression sub-lines. Interestingly, in comparison to the other sub-lines, C1 overexpression recognition levels were lower for E1ΔGA, IiE1Δ and peptide pulsed cells and the response to the peptide pulsed B18 overexpression sub-line was substantially higher. In order to confirm these results, these experiments will need to be replicated.

The Jijoye sub-lines expressing the various miRNA k/o vectors were used to compare the natural recognition of MHC class II epitopes VYG (autophagy independent) and SNP (autophagy dependent) to establish whether B18 k/o would affect CD4 T cell recognition. In comparison to the the negative controls (EV k/o and B16 k/o), the B18 k/o sub-line showed a 0.5 fold increase in IFNγ for SNP T cell recognition and a 0.2 fold increase for VYG T cell recognition. It is worth noting that the Jijoye cell lines pulsed with the cognate peptide for VYG gave very low levels of T cell recognition, especially in the case of the EV k/o line, when compared to the other two sub-lines. The VYG T cell clone was originally isolated from a Caucasian donor and had previously been shown to recognise DR11 restricted cells from an Asian donor of a different DR11 subtype. The Jijoye cell line was established from an African child with Burkitt's lymphoma and was therefore likely to carry a different subtype of DR11 which may exhibit a reduced ability to stimulate this VYG T cell clone. This may explain why the peptide pulsing for the Jijoye cell line proved to be very inefficient for VYG T cell recognition. From these results it is difficult to form a solid conclusion, as the IFNγ production in response to the physiological levels of EBNA1 expressed by the Jijoye sub-lines was relatively low and the 0.5 fold increase in IFNγ levels was therefore only a relatively small absolute change (approximately 50pg/ml). To explore whether this effect of BART 18 k/o on T cell recognition is real it would be necessary to overexpress

nuclear EBNA1 in the Jijoye sublines, as this would increase the T cell recognition levels but not alter the processing pathway of epitopes presented by the B cells [45].

4.3 EBNA1 Inhibition

The goal of immunotherapeutic treatment is to create an immune response against a given target. One way to do this is by manipulating the effector cells (activating or introducing specific T cells), while another possibility is to manipulate the target cells to make them more visible to the immune system. In the context of altering EBV infected cells, introducing dominant-negative EBNA1 proteins has been shown to alter EBNA1 processing, resulting in increased levels of MHC class I presentation and enhanced levels of T cell recognition [52]. Unfortunately, technical limitations make the clinical application of these proteins currently unfeasible. A more realistic treatment option could arise from the use of small peptides as pharmacological inhibitors of EBNA1 dimerisation, which are currently being developed by several groups [54]. Until now, pharmacological inhibition of EBNA1 dimerisation has not been investigated as a method of manipulating T cell recognition.

4.3.1 The effect of JLP2 EBNA1 inhibition on CD4 T cell recognition

JLP2 is a fluorescent EBNA1 dimerisation inhibitor that has been shown to selectively visualise and reduce the viability of an EBV-positive NPC cell line *in vitro* [55]. The collaborating laboratory (G. Wong, Hong Kong Baptist University) provided me with both JLP1 and JLP2 peptides for use in experiments exploring their specific effects on visualisation, viability and CD4 T cell recognition of EBV-positive cell lines.

The initial experiment I conducted attempting to replicate the specific visualisation of EBNA1 was unsuccessful in showing a clear distinction between EBV-positive and negative cell lines treated with JLP1 or JLP2. The results demonstrated that both peptides have non-specific binding (despite numerous washes) and fluorescence (even in the absences of cells) which raised the concern of potential non-specific effects resulting from these interactions. More

promising results were obtained using the quantifiable method of flow cytometry analysis, where it was possible to gate exclusively on cells by forward/side scatter analysis. Here, a small but observable increase in fluorescence intensity was seen for EBV-positive LCLs (B cells), but not for the EBV-negative B cells treated with JLP2 (20μM). Lower doses of JLP2 (5μM) were not sufficient to induce the increase in fluorescence for either of the EBV-positive LCLs. This result indicated that high concentrations of JLP2 are required to generate observable detection of EBV-positive B cell lines. These fluorescence intensity increases for LCLs appear to be smaller in comparison to the results of the previously published data that treated EBV-positive NPC cell lines with JLP2 [55]. This could potentially indicate different levels of EBNA1 expression or different levels of JLP2 internalisation for various cell lines. Future development of EBNA1 inhibitors will need to focus on achieving efficient internalisation of peptides to effectively inhibit EBNA1 at low doses.

In the previous publication reporting JLP2, the EBV-positive NPC (C666.1) and EBV-negative epithelial (HeLa) cell lines treated with the compound originated from different backgrounds. Although promising preliminary data was produced, the effect of JLP2 on cell viability cannot be critically assessed as it is not known whether these very different cell types would respond differently to the peptide treatment, regardless of EBV infection status. For this study I therefore chose four B cell lines, two EBV-positive and two EBV-negative, to compare cell viability upon treatment with JLP2 in similar cell backgrounds. A WST-1 (cell proliferation) assay demonstrated a JLP2 dose dependent negative effect on the cell viability for one of the EBV-positive B cells (LCL (GT)). However, this effect was only transitory, with the impact on cell viability seen at 4 hours, reduced after 24h and lost after 48h. While it does not appear as though the JLP2 detrimentally affected EBV-negative lines, it also did not affect the cell viability of the second EBV-positive B cell line (LCL (GS)). Here it may be possible to draw a link between LCL (GT),

which was shown to have the greater increase in MFI (shown in the last experiment) compared to LCL (GS), indicating that the former has higher levels of JLP2 internalisation. This difference in JLP2 internalisation may account for the differences in viability observed. This experiment still requires replication in order to validate the result. However, these results from LCL (GT) do not contradict the previously published data, in which an NPC cell line displayed a JLP2 dose dependent cell viability reduction 12h after treatment and no long term effects of JLP2 treatment were shown. A mechanism explaining why an EBNA1 inhibitor would cause such an immediate yet transitory effect on cell viability is unknown; potentially, cells are reliant on the presence of functional EBNA1 to administer its known effects on cell immortalisation and removing EBNA1 may therefore sensitise cells to apoptosis. The long term treatment with specific EBNA1 DNA binding inhibitors leads to the gradual removal of the EBV episome from cells as they divide, retarding the growth of EBV-positive cells (in comparison to EBV-negative cell growth). However, this process takes six to seven days before producing a noticeable difference [63]. EBNA1 dimerisation inhibition with JLP2 may potentially have the same long term impact. However, this requires further investigation.

Finally, I was interested in exploring the effect of EBNA1 dimerisation inhibition on epitope presentation to CD4 T cells, given that the inhibition of dimerisation could potentially increase protein degradation levels. The results here demonstrated that for both autophagy dependent and independent epitopes, only a very slight increase in CD4 T cell recognition of LCLs was seen upon treatment with JLP2 and that this effect was not dose dependent. From this data, it can be concluded that it is unlikely that the 72h treatment with JLP2 had a significant effect on the antigen processing and presentation of EBNA1 by MHC class II. Future work could investigate this in other cell types such as EBV-positive epithelial cells and could also explore the effect of JLP2 on MHC class I presentation.

4.4 Final discussion and future work

In this study I demonstrated that supraphysiological levels of both nuclear and cytoplasmic-EBNA1 were stable in the transfected epithelial cell lines that possessed high levels of basal autophagy. This contradicts a previous report published by Tellam *et al.* regarding epithelial cells, but is in accordance with the previous data exploring EBNA1 stability in B cells. My results go on to show that epithelial cells, once treated with IFNγ, were also similar to B cells in terms of EBNA1 epitope presentation to CD4 T cells. In B cells, CD4 T cell recognition of EBNA1 variants (with different abilities to access the MHC class II processing system) shows a hierarchy, which is maintained in epithelial cells (with a few exceptions). The low levels of EBNA1 degradation are nevertheless sufficient to elicit CD4 T cell recognition of epithelial cells as well as B cells. The expression of miRNA BART 18 k/o in an EBV-positive B cell line appears to slightly improve the recognition of autophagy dependent EBNA1 epitopes by CD4 T cells. However, the data from measuring autophagy levels suggests that the BART 18 only suppresses the increase in autophagy levels brought about by serum starvation. The results from an EBV-negative cell line overexpressing BART 18 did not reflect these results; it could therefore be possible that this mechanism requires multiple miRNA synergy. The treatment of cells with an EBNA1 inhibitor, JLP2, showed selective fluorescence in EBV-positive B cells, but did not greatly impact the level of T cell recognition. The treatment of B cells with JLP2 also showed an immediate yet transitory effect on cell viability and the inconsistence seen between EBV-positive cell lines may be explained by the different levels of drug uptake.

This MRes project offers the first examination of the ability of EBNA1-specific CD4 T cells to recognise epithelial cells. Despite the low levels of EBNA1 degradation observed, it is important to note that there was a degree of CD4 T cell recognition of the natural levels of EBNA1

expressed by the EBV-positive gastric carcinoma cell line MKN28 (once transfected with the appropriate HLA-molecule to match the CD4 T cell and treated with IFNγ to upregulate MHC class II presentation). This result shows that naturally expressed by EBNA1 can be present on the cell surface and could therefore be a potential target for immunotherapy in a clinical setting, although more sensitive T cell effectiveness would likely be required to elicit high levels of T cell recognition. Such effectors have recently been generated (C. Munz, personal communication) and future work using such cells could investigate the mechanisms of how different EBNA1 epitopes are processed and presented. Through studying the different epitope processing mechanisms, this research could determine the importance of autophagy or other endogenous pathways. Furthermore, higher avidity effector cells could be used to assess the role of various miRNAs, such as BART 18, on the manipulation of antigen processing and presentation, as the present data suggests that multiple factors may act in synergy to affect certain autophagy pathways. Given that different cell types appear to vary in their uptake of JLP2, it may be that epithelial lineages are more sensitive to this compound than B cell malignancies, especially as the original work on JLP2 treatment of NPC lines yielded promising results. Future work could therefore investigate the treatment of various EBV-positive and negative gastric carcinoma with EBNA1 dimerisation inhibitors for the immunotherapy of EBV-associated malignancies. Given that the majority of EBV-positive malignancies are of epithelial origin, exploring the factors that affect T cell recognition of virally encoded tumour antigens remains a priority of future work.

Supplementary figures and tables

Transfection Reagent		Cell line						
		293FT	HeLa	HaCaT	MKN1	MKN28	MKN45	NUGC4
Lipofectamine 2000	GFP (%)	84	34.6	34.9	16.1	33.4	16.5	24.1
	Cell Death (%)	17.4	4.5	0	4.8	6.5	0.7	3.1
Mirus Transit X2	GFP (%)	53.7	77.2	27.1	5.7	48.4	5.3	28.4
	Cell Death (%)	23.2	6	36	11.4	21.7	0	7.8

Table S3.1.1 Data from the comparison of transfection reagents in epithelial cell lines
The reagents Lipofectamine 2000 or Mirus Transit X2 were used to transfect the cell lines (MKN1, MKN28, MKN45, NUGC4, HeLa, 293FT and HaCaT) with 4µg/ml pCDNA3-GFP. Flow cytometry was used to assess transfection efficiency (GFP expression) and cell viability (propidium iodide staining), using mock transfected cells as a baseline reference point. Intact cells were analysed by gating on this population using forward scatter and side scatter (not shown). The results demonstrate that the cell viability was generally high (between 80-100%) for both reagents, but Lipofectamine transfections were consistently better, or as good as Muris transfection. The efficiency of transfections varied between the two reagents depending on the cell line;

CD4 T cells (IFNγ)

		Funtional					Non-functional
	T cell	GPW	SNP	AGIL	LLQ	SDD	VYG
	HLA Type	DR1	DR51	DR52b	DQ6	DQ5	DR11
Cell line	293FT	-58	-23	-41	-38	-53	-6
	HeLa	**329**	-39	**332**	-41	**29**	388
	HaCaT	-56	-21	-46	**447**	-47	248
	MKN 45	-54	**257**	**1309**	-44	-12	46
	MKN 28	-4	-37	-11	-49	-40	577
	MKN 1	-50	-45	**7720**	-41	-47	222
	T cells alone (-ve)	-39	-48	-32	-46	-40	65
	T cells + Pepties (+ve)	418	-17	4785	-25	108	6782

CD8 T cells (IFNγ)

		Funtional				Non-functional		
	T cells	GLC	YVL	RPH	HPV	RPP	AVF	IVT
	HLA type	A2	A2	B7	B35	B7	A11	A11
Cell line	293FT	**1965**	**39**	**58**	-25	-45	-45	-47
	HeLa	-51	-24	-20	-47	-42	-44	-43
	HaCaT	-48	-42	-19	-49	-37	-45	-30
	MKN45	-33	-38	-13	-46	-35	-35	-50
	MKN28	-48	-4	-19	-44	-25	-38	-45
	MKN 1	-50	-45	-29	-47	-37	-41	-54
	T cells (-ve)	-34	-40	-35	28	-35	-36	-34
	T cells + Pepties	642	170	-35	431	-44	1	-40

Table S3.2.1 Data from the analysis of HLA restriction T cell assay for epithelial cell lines
The cell lines (Hela, HaCaT, 293FT, MKN1, MKN28 and MKN45) were incubated with IFNγ for 72h to induce the expression of MHC class II. The cells were then peptide pulsed with each T cell clone's cognate peptide. A T cell assay was then performed and IFNγ release was measured using an ELISA.

Autophagy levels compared to the empty vector control

	miRNA	BART16		BART 18		Cluster 1	
	Culturing conditions	Normal	Serum stavation	Normal	Serum stavation	Normal	Serum stavation
Cell line	MJS (overexpression)	Increase	Increase	Increase	Increase	Increase	Increase
	Jijoye (k/o)	Decrease	Decrease	Equal	Increase	NA	NA

Table S3.2.2 Summary of miRNA k/o and overexpression effect on autophagy
Data summarised from LC3 fluxes, comparing the levels of autophagy seen in empty vector negative control to the levels seen in the sub-lines overexpressing or knocking out miRNA.

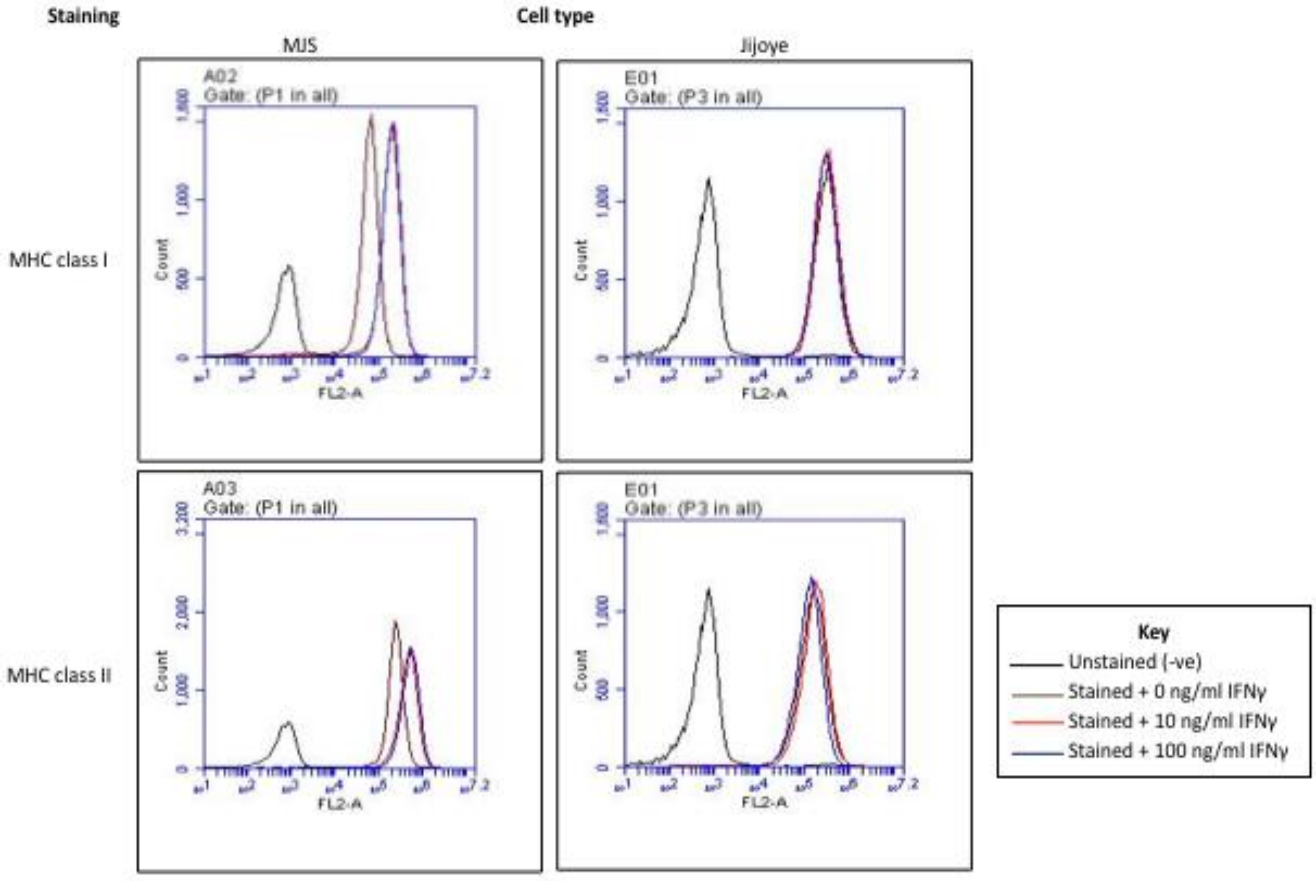

Figure S3.2.1 IFNγ Cell surface staining for MHC class I and II presentation, varying IFNγ concentrations, in Jijoye and MJS cell lines

FAC analysis of MHC class I and II surface presentation in the Jijoye (right column) and MJS (left column) cell line, cultured for 72h in different levels of IFNγ (0,10,100ng/ml). The result shows that Jijoye's MHC class I and II is not upregulated and that there is no additional upregulation in MJS when culturing in 100ng/ml ifnγ compared to 10ng/ml.

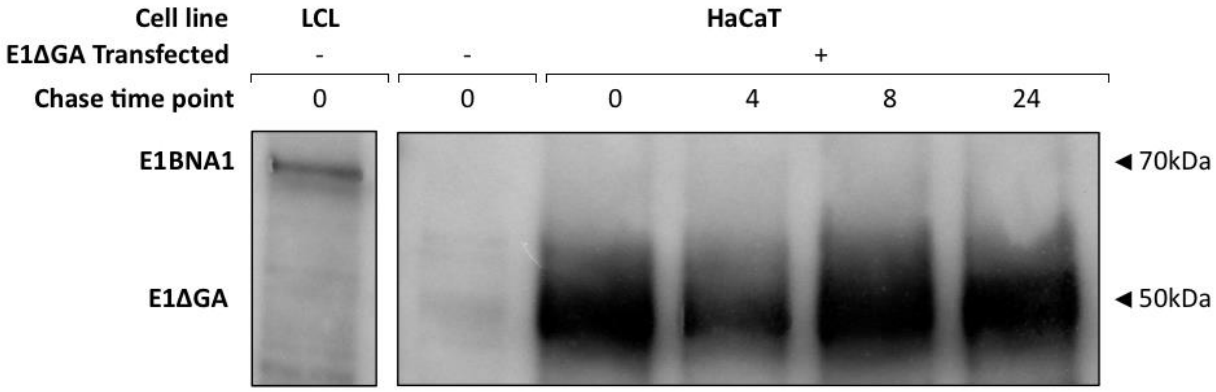

Figure S4.1.1 Analysis of E1ΔGA stability in transfected HaCaT cell lines
The HaCaT cell line was transfected with pCDNA3-E1ΔGA (4ng/ml) and cultured for 48h. Protein synthesis was then inhibited with the addition of cycloheximide (50ug/ml) and cells were chased for 0, 4, 8 and 24h. Samples were standardised and EBNA1 levels were assessed using western blotting. The consistent band intensity shown across 24h, except for the anomaly at 4h, demonstrates EBNA1 was stable in this cell line.

References

1. Parkin, D.M., *The global health burden of infection -associated cancers in the year 2002.* International Journal of Cancer, 2006. **118**(12): p. 3030-3044.
2. Alter, B.J. and F.H. Bach, *Lymphocyte reactivity in vitro. I. Cellular reconstitution of purified lymphocyte response.* Cellular immunology, 1970. **1**(2): p. 207-18.
3. Meuer, S.C., et al., *IDENTIFICATION OF THE RECEPTOR FOR ANTIGEN AND MAJOR HISTOCOMPATIBILITY COMPLEX ON HUMAN INDUCER LYMPHOCYTES-T.* Science, 1983. **222**(4629): p. 1239-1242.
4. Calderon, L. and T. Boehm, *Three chemokine receptors cooperatively regulate homing of hematopoietic progenitors to the embryonic mouse thymus.* Proceedings of the National Academy of Sciences of the United States of America, 2011. **108**(18): p. 7517-7522.
5. Koch, U., et al., *Delta-like 4 is the essential, nonredundant ligand for Notch1 during thymic T cell lineage commitment.* Journal of Experimental Medicine, 2008. **205**(11): p. 2515-2523.
6. Manfras, B.J., D. Terjung, and B.O. Boehm, *Non-productive human TCR beta chain genes represent V-D-J diversity before selection upon function: Insight into biased usage of TCRBD and TCRBJ genes and diversity of CDR3 region length.* Human Immunology, 1999. **60**(11): p. 1090-1100.
7. Biro, J., et al., *Regulation of T cell receptor (TCR) beta gene expression by CD3 complex signaling in immature thymocytes: Implications for TCR beta allelic exclusion.* Proceedings of the National Academy of Sciences of the United States of America, 1999. **96**(7): p. 3882-3887.
8. Carson, R.T., et al., *T cell receptor recognition of MHC class II-bound peptide flanking residues enhances immunogenicity and results in altered TCR V region usage.* Immunity, 1997. **7**(3): p. 387-399.
9. Blanden, R.V., et al., *GENES REQUIRED FOR CYTOTOXICITY AGAINST VIRUS-INFECTED TARGET-CELLS IN K-REGION AND D-REGION OF H-2 COMPLEX.* Nature, 1975. **254**(5497): p. 269-270.
10. Land, W.G., *Emerging role of innate immunity in organ transplantation Part II: potential of damage-associated molecular patterns to generate immunostimulatory dendritic cells.* Transplantation Reviews, 2012. **26**(2): p. 73-87.
11. Mosmann, T.R., et al., *Pillars article: Two types of murine helper T cell clone. I. Definition according to profiles of lymphokine activities and secreted proteins.* Journal of Immunology, 2005. **175**(1): p. 5-14.
12. Murphy, E., et al., *Reversibility of T helper 1 and 2 populations is lost after long-term stimulation.* Journal of Experimental Medicine, 1996. **183**(3): p. 901-913.
13. Hegazy, A.N., et al., *Interferons Direct Th2 Cell Reprogramming to Generate a Stable GATA-3(+)T-bet(+) Cell Subset with Combined Th2 and Th1 Cell Functions.* Immunity, 2010. **32**(1): p. 116-128.
14. Murphy, K.M. and B. Stockinger, *Effector T cell plasticity: flexibility in the face of changing circumstances.* Nature Immunology, 2010. **11**(8): p. 674-680.
15. Morisaki, T., et al., *CHARACTERIZATION AND AUGMENTATION OF CD4+ CYTOTOXIC T-CELL LINES AGAINST MELANOMA.* Cancer Immunology Immunotherapy, 1994. **39**(3): p. 172-178.
16. Braumueller, H., et al., *T-helper-1-cell cytokines drive cancer into senescence.* Nature, 2013. **494**(7437): p. 361-365.

17. Gil-Torregrosa, B.C., A.R. Castano, and M. Del Val, *Major histocompatibility complex class I viral antigen processing in the secretory pathway defined by the trans-Golgi network protease furin.* Journal of Experimental Medicine, 1998. **188**(6): p. 1105-1116.
18. Munz, C., *Antigen Processing for MHC Class II Presentation via Autophagy.* Frontiers in immunology, 2012. **3**: p. 9-9.
19. Steimle, V., et al., *REGULATION OF MHC CLASS-II EXPRESSION BY INTERFERON-GAMMA MEDIATED BY THE TRANSACTIVATOR GENE CIITA.* Science, 1994. **265**(5168): p. 106-109.
20. Rammensee, H.G., et al., *SYFPEITHI: database for MHC ligands and peptide motifs.* Immunogenetics, 1999. **50**(3-4): p. 213-219.
21. Dengjel, J., et al., *Autophagy promotes MHC class II presentation of peptides from intracellular source proteins.* Proceedings of the National Academy of Sciences of the United States of America, 2005. **102**(22): p. 7922-7927.
22. Jung, C.H., et al., *ULK-Atg13-FIP200 Complexes Mediate mTOR Signaling to the Autophagy Machinery.* Molecular Biology of the Cell, 2009. **20**(7): p. 1992-2003.
23. Itakura, E. and N. Mizushima, *Characterization of autophagosome formation site by a hierarchical analysis of mammalian Atg proteins.* Autophagy, 2010. **6**(6): p. 764-776.
24. Lamark, T. and T. Johansen, *Aggrephagy: selective disposal of protein aggregates by macroautophagy.* International journal of cell biology, 2012. **2012**: p. 736905-736905.
25. Paludan, C., et al., *Endogenous MHC class II processing of a viral nuclear antigen after autophagy.* Science, 2005. **307**(5709): p. 593-596.
26. Schmid, D., M. Pypaert, and C. Munz, *Antigen-loading compartments for major histocompatibility complex class II molecules continuously receive input from autophagosomes.* Immunity, 2007. **26**(1): p. 79-92.
27. Comber, J.D., et al., *Functional Macroautophagy Induction by Influenza A Virus without a Contribution to Major Histocompatibility Complex Class II-Restricted Presentation.* Journal of Virology, 2011. **85**(13): p. 6453-6463.
28. Dishop, M.K. and S. Kuruvilla, *Primary and metastatic lung tumors in the pediatric population - A review and 25-year experience at a large children's hospital.* Archives of Pathology & Laboratory Medicine, 2008. **132**(7): p. 1079-1103.
29. Penn, I. and T.E. Starzl, *MALIGNANT TUMORS ARISING DE NOVO IN IMMUNOSUPPRESSED ORGAN TRANSPLANT RECIPIENTS.* Transplantation, 1972. **14**(4): p. 407-&.
30. Griffin, B.D., M.C. Verweij, and E.J.H.J. Wiertz, *Herpesviruses and immunity: The art of evasion.* Veterinary Microbiology, 2010. **143**(1): p. 89-100.
31. Rooney, C.M., et al., *Adoptive transfer of polyclonal, EBV-specific cytotoxic T-cell lines for the prevention and treatment of EBV-associated malignancies*. Cell Therapy, ed. Y. Ikeda, et al. Vol. 5. 2000. 45-60.
32. Klebanoff, C.A., L. Gattinoni, and N.P. Restifo, *Sorting Through Subsets: Which T-Cell Populations Mediate Highly Effective Adoptive Immunotherapy?* Journal of Immunotherapy, 2012. **35**(9): p. 651-660.
33. Haque, T., et al., *Allogeneic cytotoxic T-cell therapy for EBV-positive posttransplantation lymphoproliferative disease: results of a phase 2 multicenter clinical trial.* Blood, 2007. **110**(4): p. 1123-1131.
34. Perez-Diez, A., et al., *CD4 cells can be more efficient at tumor rejection than CD8 cells.* Blood, 2007. **109**(12): p. 5346-5354.
35. Hunder, N.N., et al., *Treatment of metastatic melanoma with autologous CD4+T cells against NY-ESO-1.* New England Journal of Medicine, 2008. **358**(25): p. 2698-2703.

36. Hislop, A.D., et al., *Cellular responses to viral infection in humans: Lessons from Epstein-Barr virus*, in *Annual Review of Immunology*. 2007. p. 587-617.
37. Thorley-Lawson, D.A., K.A. Duca, and M. Shapiro, *Epstein-Barr virus: a paradigm for persistent infection - for real and in virtual reality.* Trends in Immunology, 2008. **29**(4): p. 195-201.
38. Thorley-Lawson, D.A. and A. Gross, *Mechanisms of disease - Persistence of the Epstein-Barr virus and the origins of associated lymphomas.* New England Journal of Medicine, 2004. **350**(13): p. 1328-1337.
39. Marquitz, A.R., et al., *Expression Profile of MicroRNAs in Epstein-Barr Virus-Infected AGS Gastric Carcinoma Cells.* Journal of Virology, 2014. **88**(2): p. 1389-1393.
40. Bornkamm, G.W. and W. Hammerschmidt, *Molecular virology of Epstein-Barr virus.* Philosophical Transactions of the Royal Society of London Series B-Biological Sciences, 2001. **356**(1408): p. 437-459.
41. Humme, S., et al., *The EBV nuclear antigen 1 (EBNA1) enhances B cell immortalization several thousandfold.* Proceedings of the National Academy of Sciences of the United States of America, 2003. **100**(19): p. 10989-10994.
42. Cohen, J.I., et al., *Epstein-Barr Virus: An Important Vaccine Target for Cancer Prevention.* Science Translational Medicine, 2011. **3**(107).
43. Hui, E.P., et al., *Phase I Trial of Recombinant Modified Vaccinia Ankara Encoding Epstein-Barr Viral Tumor Antigens in Nasopharyngeal Carcinoma Patients.* Cancer Research, 2013. **73**(6): p. 1676-1688.
44. Reisman, D. and B. Sugden, *TRANS ACTIVATION OF AN EPSTEIN-BARR VIRAL TRANSCRIPTIONAL ENHANCER BY THE EPSTEIN-BARR VIRAL NUCLEAR ANTIGEN-1.* Molecular and Cellular Biology, 1986. **6**(11): p. 3838-3846.
45. Leung, C.S., et al., *Nuclear location of an endogenously expressed antigen, EBNA1, restricts access to macroautophagy and the range of CD4 epitope display.* Proceedings of the National Academy of Sciences of the United States of America, 2010. **107**(5): p. 2165-2170.
46. Tellam, J., et al., *Targeting of EBNA1 for rapid intracellular degradation overrides the inhibitory effects of the Gly-Ala repeat domain and restores CD8+T cell recognition.* Journal of Biological Chemistry, 2001. **276**(36): p. 33353-33360.
47. Tellam, J., et al., *Endogenous presentation of CD8(+) T cell epitopes from Epstein-Barr virus-encoded nuclear antigen 1.* Journal of Experimental Medicine, 2004. **199**(10): p. 1421-1431.
48. Long, H.M., et al., *CD4(+) T-cell responses to Epstein-Barr virus (EBV) latent-cycle antigens and the recognition of EBV-transformed lymphoblastoid cell lines.* Journal of Virology, 2005. **79**(8): p. 4896-4907.
49. Munz, C., et al., *Human CD4(+) T lymphocytes consistently respond to the latent Epstein-Barr virus nuclear antigen EBNA1.* Journal of Experimental Medicine, 2000. **191**(10): p. 1649-1660.
50. Dantuma, N.P., A. Sharipo, and M.G. Masucci, *Avoiding proteasomal processing: The case of EBNA1.* Viral Proteins Counteracting Host Defenses, 2002. **269**: p. 23-36.
51. Paludan, C., et al., *Epstein-Barr nuclear antigen 1-specific CD4(+) Th1 cells kill Burkitt's lymphoma cells.* Journal of Immunology, 2002. **169**(3): p. 1593-1603.
52. Jones, R.J., et al., *Epstein-Barr virus nuclear antigen 1 (EBNA1) induced cytotoxicity in epithelial cells is associated with EBNA1 degradation and processing.* Virology, 2003. **313**(2): p. 663-676.
53. Imai, S., et al., *Therapeutic inhibition of Epstein-Barr virus-associated tumor cell growth by dominant-negative EBNA1.* Uirusu, 2005. **55**(2): p. 239-49.

54. Kim, S.Y., et al., *Small molecule and peptide-mediated inhibition of Epstein-Barr virus nuclear antigen 1 dimerization.* Biochemical and Biophysical Research Communications, 2012. **424**(2): p. 251-256.
55. Jiang, L., et al., *EBNA1-specific luminescent small molecules for the imaging and inhibition of latent EBV-infected tumor cells.* Chemical Communications, 2014. **50**(49): p. 6517-6519.
56. Mizushima, N. and T. Yoshimori, *How to interpret LC3 immunoblotting.* Autophagy, 2007. **3**(6): p. 542-545.
57. Thelemann, C., et al., *Interferon-gamma Induces Expression of MHC Class II on Intestinal Epithelial Cells and Protects Mice from Colitis.* Plos One, 2014. **9**(1).
58. Zuo, J., et al., *Kaposi's Sarcoma-Associated Herpesvirus-Encoded Viral IRF3 Modulates Major Histocompatibility Complex Class II (MHC-II) Antigen Presentation through MHC-II Transactivator-Dependent and -Independent Mechanisms: Implications for Oncogenesis.* Journal of Virology, 2013. **87**(10): p. 5340-5350.
59. Stacey, K.J., I.L. Ross, and D.A. Hume, *ELECTROPORATION AND DNA-DEPENDENT CELL-DEATH IN MURINE MACROPHAGES.* Immunology and Cell Biology, 1993. **71**: p. 75-85.
60. Larsen, S.L., et al., *T cell responses affected by aminopeptidase N (CD13)-mediated trimming of major histocompatibility complex class II-bound peptides.* Journal of Experimental Medicine, 1996. **184**(1): p. 183-189.
61. Linnstaedt, S.D., et al., *Virally Induced Cellular MicroRNA miR-155 Plays a Key Role in B-Cell Immortalization by Epstein-Barr Virus.* Journal of Virology, 2010. **84**(22): p. 11670-11678.
62. Xu, J., et al., *MiRNA-miRNA synergistic network: construction via co-regulating functional modules and disease miRNA topological features.* Nucleic Acids Research, 2011. **39**(3): p. 825-836.
63. Lee, E.K., et al., *Small molecule inhibition of Epstein-Barr virus nuclear antigen-1 DNA binding activity interferes with replication and persistence of the viral genome.* Antiviral Research, 2014. **104**: p. 73-83.